



1 Global biogeography of N₂-fixing microbes: *nifH* amplicon database 2 and analytics workflow

3 Michael Morando^{1*}, Jonathan Magasin^{1*}, Shunyan Cheung^{1,2}, Matthew M. Mills³, Jonathan P. Zehr¹,
4 Kendra A. Turk-Kubo¹

5 ¹Ocean Sciences Department, University of California, Santa Cruz, Santa Cruz, 95064, United States

6 ²Institute of Marine Biology and Center of Excellence for the Oceans, National Taiwan Ocean University, Keelung, Taiwan

7 ³Earth System Science, Stanford University, Stanford, 94305, United States

8 * equal contributions

9 Correspondence to: Kendra A. Turk-Kubo (kturk@ucsc.edu)

10 **Abstract.** Marine nitrogen (N) fixation is a globally significant biogeochemical process carried out by a specialized group of
11 prokaryotes (diazotrophs), yet our understanding of their ecology is constantly evolving. Although marine dinitrogen (N₂)-
12 fixation is often ascribed to cyanobacterial diazotrophs, indirect evidence suggests that non-cyanobacterial diazotrophs (NCDs)
13 might also be important. One widely used approach for understanding diazotroph diversity and biogeography is polymerase
14 chain reaction (PCR)-amplification of a portion of the *nifH* gene, which encodes a structural component of the N₂-fixing
15 enzyme complex, nitrogenase. An array of bioinformatic tools exists to process *nifH* amplicon data, however, the lack of
16 standardized practices has hindered cross-study comparisons. This has led to a missed opportunity to more thoroughly assess
17 diazotroph biogeography, diversity, and their potential contributions to the marine N cycle. To address these knowledge gaps
18 a bioinformatic workflow was designed that standardizes the processing of *nifH* amplicon datasets originating from high-
19 throughput sequencing (HTS). Multiple datasets are efficiently and consistently processed with a specialized DADA2 pipeline
20 to identify amplicon sequence variants (ASVs). A series of customizable post-pipeline stages then detect and discard spurious
21 *nifH* sequences and annotate the subsequent quality-filtered *nifH* ASVs using multiple reference databases and classification
22 approaches. This newly developed workflow was used to reprocess nearly all publicly available *nifH* amplicon HTS datasets
23 from marine studies, and to generate a comprehensive *nifH* ASV database containing 7909 ASVs aggregated from 21 studies
24 that represent the diazotrophic populations in the global ocean. For each sample, the database includes physical and chemical
25 metadata obtained from the Simons Collaborative Marine Atlas Project (CMAP). Here we demonstrate the utility of this
26 database for revealing global biogeographical patterns of prominent diazotroph groups and highlight the influence of sea
27 surface temperature. The workflow and *nifH* ASV database provide a robust framework for studying marine N₂ fixation and
28 diazotrophic diversity captured by *nifH* amplicon HTS. Future datasets that target understudied ocean regions can be added
29 easily, and users can tune parameters and studies included for their specific focus. The workflow and database are available,
30 respectively, in GitHub (<https://github.com/jdmagasin/nifH-ASV-workflow>; Morando et al., 2024) and Figshare
31 (<https://doi.org/10.6084/m9.figshare.23795943.v1>; Morando et al., 2024).



32 1 Introduction

33 Dinitrogen (N₂) fixation, the reduction of N₂ into bioavailable NH₃ is a source of new nitrogen (N) in the oceans and can
34 support as much as 70% of new primary production in N-limited oligotrophic gyres (Jickells et al., 2017). Over millennia, N₂
35 fixation may balance the loss of N from the marine system through denitrification and annamox (Zehr and Capone, 2020). N₂
36 fixation was thought to be performed exclusively by prokaryotes, yet it was recently demonstrated that the marine haptophyte
37 alga, *Braarudosphaera bigelowii*, contains a cyanobacterially-derived organelle specialized for N₂ fixation (Coale et al., 2024).
38 Noting this exception, microorganisms able to fix N₂ (diazotrophs), are broadly characterized into two main groups,
39 cyanobacterial diazotrophs (those phylogenetically related to cyanobacteria) and non-cyanobacterial diazotrophs (NCDs).
40 Historically, cyanobacterial diazotrophs have been considered the most important contributors to marine N₂ fixation (Villareal,
41 1994; Capone et al., 2005). NCDs, first detected by Zehr et al. (1998), have since been demonstrated to be ubiquitous in pelagic
42 marine waters, and are generally thought to be putative chemoheterotrophs with a highly diverse lineage that includes the
43 massive phylum Proteobacteria as well as Firmicutes, Actinobacteria, and Chloroflexi (Turk-Kubo et al., 2022). However,
44 their contribution of fixed N and their role in the global ocean is not well-understood (Moisander et al., 2017).

45
46 Diazotrophs are often present at low abundances relative to other members of ocean microbiomes, which makes them
47 challenging to study (Moisander et al., 2017; Benavides et al.). Distinctive pigments and morphologies that enable some
48 cyanobacterial diazotrophs to be identified by microscopy are lacking in many diazotrophs (Carpenter and Capone, 1983;
49 Carpenter and Foster, 2002), including NCDs. Furthermore, many marine diazotrophs are uncultivated, which has required the
50 use of cultivation-independent approaches such as PCR and quantitative PCR (qPCR) (Luo et al., 2012; Shao and Luo, 2022;
51 Turk-Kubo et al., 2022). The *nifH* gene encodes the identical subunits of the Fe protein of nitrogenase, the enzyme that
52 catalyzes the N₂ fixation reaction, and contains both highly conserved and variable regions enabling its use as a phylogenetic
53 marker and as a proxy for N₂-fixing potential in marine ecosystems globally (Gaby and Buckley, 2011).

54
55 Although the importance of marine N₂ fixation is well-established, knowledge gaps remain, and discoveries continue to be
56 made (Zehr and Capone, 2020). For example, high-throughput sequencing (HTS) of *nifH* amplicons is expanding our
57 knowledge of diazotroph biogeography and activity and has revealed surprising new diversity. However, HTS studies often
58 utilize different or custom software pipelines and parameters, rendering direct comparisons between studies difficult.
59 Additionally, many studies do not address the full breadth of diazotrophic diversity because they focus on cyanobacterial
60 diazotrophs while providing only a superficial analysis of the NCDs present. The resulting lack of information on NCD *in situ*
61 distributions limits our understanding of diazotroph ecology and N₂ fixation as well as our ability to predict how these
62 populations will respond, e.g., trait-based ecological models, to a continually changing ocean.

63
64 To address these issues, we compiled published *nifH* amplicon HTS datasets along with two new datasets. Twenty-one studies
65 were reprocessed by our newly developed software workflow, which streamlines the integration of multiple, large amplicon



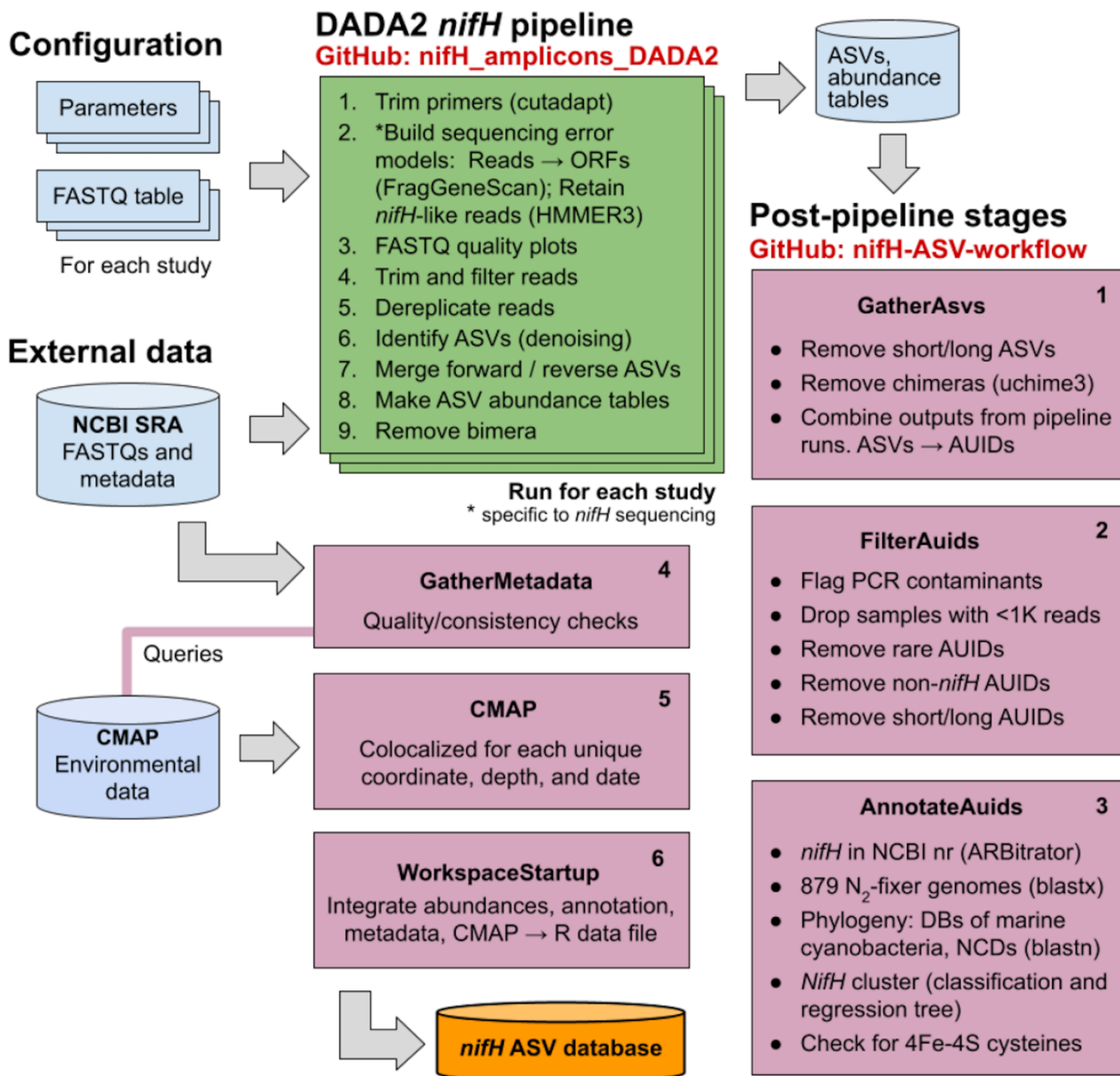
66 datasets for reproducible analyses. The workflow identifies amplicon sequence variants (ASVs) using a pipeline developed
67 around DADA2 (Callahan et al., 2016) — the DADA2 *nifH* pipeline — and then executes rigorous post-pipeline stages to:
68 remove spurious *nifH* ASVs; annotate the remaining quality-filtered ASVs using multiple reference databases and
69 classification approaches; and obtain *in situ* and modeled environmental data for each sample from the Simons Collaborative
70 Marine Atlas Project (CMAP; <https://simonscmap.com>). Although created to support research into N₂ fixation (*nifH*), the
71 complete workflow (ASV pipeline followed by the post-pipeline stages) can be adapted for use with other amplicon datasets,
72 including other functional genes or taxonomic markers (16S rRNA genes), with some simple modifications.

73
74 In addition to the workflow, our efforts resulted in the construction of a comprehensive database of *nifH* ASVs with contextual
75 metadata that will be a community resource for marine diazotroph investigations, enhancing comparability between previous
76 and future *nifH* amplicon datasets. The *nifH* ASV database is available in Figshare
77 (<https://doi.org/10.6084/m9.figshare.23795943.v1>; Morando et al., 2024). The entire workflow required to produce the *nifH*
78 ASV database is available in two GitHub repositories, the DADA2 *nifH* pipeline
79 (https://github.com/jdmagasin/nifH_amplicons_DADA2), and the post-pipeline stages ([https://github.com/jdmagasin/nifH-](https://github.com/jdmagasin/nifH-ASV-workflow)
80 [ASV-workflow](https://github.com/jdmagasin/nifH-ASV-workflow); Morando et al., 2024).

81 **2 Data and Methods**

82 **2.1 Overview of *nifH* amplicon workflow and *nifH* ASV database generation**

83 The full workflow is comprised of two parts: 1) the DADA2 *nifH* pipeline; and 2) a series of post-pipeline stages (Fig. 1).
84
85



86
 87
 88
 89
 90
 91
 92
 93
 94
 95

Figure 1: Schematic of the *nifH* amplicon data workflow. Data from all studies that met our criteria (Sect. 2.2) were downloaded from the NCBI Sequence Read Archive (SRA) and processed separately through the DADA2 *nifH* pipeline (green; Sect. 2.3.2), generally using identical parameters. ASV sequences and abundance tables from all studies were then combined and processed through each stage of the post-pipeline workflow (purple, Sect. 2.3.3) by executing the Makefile associated with each stage. Post-pipeline stages quality-filtered and then annotated the ASVs by reference to several *nifH* databases, and downloaded CMAP environmental data matched to the date, coordinates, and depth of each amplicon dataset. The main output of the entire workflow (pipeline and post-pipeline) is the *nifH* ASV database, which is available in Figshare (<https://doi.org/10.6084/m9.figshare.23795943.v1>; Morando et al., 2024). The workflow is maintained in two GitHub repositories, one for the DADA2 *nifH* pipeline (https://github.com/jdmagasin/nifH_amplicons_DADA2) and one for the post-pipeline stages (<https://github.com/jdmagasin/nifH-ASV-workflow>; Morando et al., 2024).



96

97

98 Required inputs for the pipeline are raw *nifH* amplicon sequencing reads and sample collection metadata (at minimum the
99 latitude and longitude, depth and sample collection date and time) used to acquire environmental metadata from CMAP.
100 Criteria for including publicly available datasets are detailed in Section 2.2.1.

101

102 The DADA2 software package is frequently used for processing 16/18S rRNA gene amplicon sequencing data due to its ability
103 to remove base calling errors (“denoising”) and thereby infer error-free ASVs (Callahan et al., 2016). We have developed a
104 customizable pipeline to improve the error models utilized by DADA2 by training them only on reads in a dataset that are
105 valid *nifH* sequences (not PCR artifacts). The DADA2 pipeline runs from the command line in a Unix-like shell, moving
106 through nine steps (Fig. 1 DADA2 *nifH* pipeline) described in Section 2.3.2 for each study independently. After the DADA2
107 pipeline is completed, outputs from all studies are integrated and refined by the six post-pipeline stages of the workflow, which
108 perform additional quality filtering (e.g., size- and abundance-based selection), identify and remove spurious sequences (e.g.,
109 potential contaminants and non-target sequences), and annotate the ASVs (Fig. 1 Post-pipeline stages). By considering ASVs
110 from all studies simultaneously, the workflow considers rare ASVs that might be discarded as irrelevant in a single-study
111 analysis. Workflow stages are executed manually by running their associated Makefiles and Snakefiles within a Unix-like
112 shell.

113

114 The workflow generates the final data product published in this work, the *nifH* ASV database, which includes ASV sequences,
115 abundance and annotation tables, sample collection metadata, and sample environmental data from CMAP (Fig. 1). The
116 database is available in Figshare (<https://doi.org/10.6084/m9.figshare.23795943.v1>; Morando et al., 2024) as a set of tables
117 (comma-separated value files) and an ASV FASTA file. However, these are also provided within an R data file,
118 workspace.RData, in the WorkspaceStartup directory in the workflow GitHub repository, for users who wish to analyze, curate,
119 or customize the database using R packages for ecological analysis. All documentation, scripts, and data needed to run the
120 workflow and produce the *nifH* ASV database are provided in the workflow GitHub repository
121 (<https://github.com/jdmagasin/nifH-ASV-workflow>; Morando et al., 2024). This includes pre-generated pipeline results for
122 each of the 21 studies as well as the pipeline parameters files.

123

124 In summary, the workflow facilitates the systematic and reproducible exploration of *nifH*-based diversity within microbial
125 communities and was applied to available *nifH* amplicon data to generate a globally distributed *nifH* ASV database. Together
126 the workflow and *nifH* ASV database will serve as valuable community resources, fostering future investigations while
127 ensuring comparability between previous and forthcoming studies. In the following sections, detailed descriptions of each
128 stage of the workflow are provided.

129



130 **2.2 Compilation of *nifH* amplicon studies**

131 **2.2.1 Published studies**

132 We compiled all publicly available *nifH* amplicon HTS data that were generated using the *nifH*1-4 primers (Zani, 1999; Zehr
 133 and McCreynolds, 1989) and subsequently sequenced on the Illumina MiSeq/HiSeq platform totaling 19 studies (Table 1).
 134 Limiting the scope to investigations that used the same amplification primers enabled a more tractable comparison across
 135 studies by different research groups that employed varying approaches to sample collection and preparation for sequencing by
 136 different centers. Datasets were downloaded directly from the National Center for Biotechnology Information (NCBI)
 137 Sequencing Read Archive (SRA) using the GrabSeqs tool (Taylor et al., 2020) by specifying the study's NCBI project
 138 accession. Each dataset obtained included paired-end sequencing reads (in FASTQ files) and a table with the collection
 139 metadata for each sample. Some datasets could not be retrieved directly from the SRA and were obtained directly from the
 140 authors (Table A1). Note that we did not include studies where data was generated from experimental perturbations or particle
 141 enrichments (Table A1). Data were last accessed from NCBI SRA on 17 April 2024.

142
 143 **Table 1: Information on the studies compiled to generate the *nifH* ASV database.** All compiled studies and associated information.
 144 This includes the study ID used to refer to each dataset, the number of samples, NCBI BioProject accession, a reference to each publication
 145 and its corresponding DOI.

146

Study ID	Samples	NCBI BioProject	Reference	DOI
AK2HI	43	PRJNA1062410	This study	n/a
BentzonTilia_2015	56	PRJNA239310	Bentzon-Tilia et al., 2015	10.1038/ismej.2014.119
Ding_2021	32	SUB7406573	Ding et al., 2021	10.3390/biology10060555
Gradoville_2020_G1	111	PRJNA530276	Gradoville et al., 2020	10.1002/lno.11423
Gradoville_2020_G2	56	PRJNA530276	Gradoville et al., 2020	10.1002/lno.11423
Hallstrom_2021	82	PRJNA656687	Hallstrøm et al., 2022b	10.1002/lno.11997
Hallstrom_2022	83	PRJNA756869	Hallstrøm et al., 2022a	10.1007/s10533-022-00940-w
Harding_2018	91	PRJNA476143	Harding et al., 2018	10.1073/pnas.1813658115
Mulholland_2018	29	PRJNA841982	Mulholland et al., 2019	10.1029/2018GB006130
NEMO	56	PRJNA1062391	This study	n/a
Raes_2020	121	PRJNA385736	Raes et al., 2020	10.3389/fmars.2020.00389
Sato_2021	28	PRJDB10819	Sato et al., 2021	10.1029/2020JC017071
Selden_2021	10	PRJNA683637	Selden et al., 2021	10.1002/lno.11727
Shiozaki_2017	22	PRJDB5199	Shiozaki et al., 2017	10.1002/2017GB005681
Shiozaki_2018GBC	20	PRJDB6603	Shiozaki et al., 2018b	10.1029/2017GB005869
Shiozaki_2018LNO	20	PRJDB5679	Shiozaki et al., 2018a	10.1002/lno.10933



Shiozaki_2020	14	PRJDB9222	Shiozaki et al., 2020	10.1038/s41561-020-00651-7
Tang_2020	6	PRJNA554315	Tang et al., 2020	10.1038/s41396-020-0703-6
TianjUni_2016	14	PRJNA637983	Wu et al., 2021	10.1007/s10021-021-00702-z
TianjUni_2017	18	PRJNA438304	Wu et al., 2019	10.1007/s00248-019-01355-1
Turk_2021	136	PRJNA695866	Turk-Kubo et al., 2021	10.1038/s43705-021-00039-7

147
148

149

150

151

152

153

154

155

156

157

158

159

160

161

162

163

164

165

166

167

168

169

170

171

172

173

174

175

Sample quality was validated prior to processing through the DADA2 *nifH* pipeline. Samples were discarded if they did not contain unmerged pairs of forward and reverse reads with properly oriented primer sequences (Table A1). There were two exceptions, studies by Shiozaki et al. (2017) and Shiozaki et al. (2018b), that used mixed-orientation sequence libraries and required preprocessing. The reads in each of these studies were partitioned by whether they captured the coding or template strand of *nifH*, determined by primer orientation. Because HTS sequence quality generally degrades from 5' to 3', the partitioned data were run separately through the pipeline to preserve their sequencing error profiles for DADA2. The ASVs from the misoriented reads (e.g. forward reads with template sequence) were then reverse-complemented and combined with the properly oriented ASVs into a single ASV abundance table and FASTA file. Table 1 and Table A1 provide information for obtaining the raw FASTQ files for all samples evaluated for the *nifH* ASV database including information regarding studies excluded from the database.

2.2.2 Unpublished *nifH* amplicon datasets

Additional *nifH* gene HTS datasets were included from DNA samples collected on two cruises in the North Pacific. One was a transect cruise across the Eastern North Pacific (NEMO; R/V New Horizon, August 2014; Shilova et al., 2017), and the other was a transect cruise from Alaska to Hawaii (AK2HI; R/V Kilo Moana, September 2017). Euphotic zone samples were collected from Niskin bottles deployed on a CTD-rosette (NEMO) or from the underway water system (5 m; AK2HI). NEMO samples (2-4 L) were filtered through 0.2 μm and 3 μm pore-size filters (in series), while AK2HI samples (ca. 2 L) were filtered through 0.2 μm pore-size filters using gentle peristaltic pumping. Filters were dried, flash frozen and stored at -80°C until processing. DNA was extracted using a modified DNeasy Plant Kit (Qiagen, Germantown, MD) protocol, described in detail in Moisaner et al. (2008), with on-column washing steps automated by a QIAcube (Qiagen).

Partial *nifH* DNA sequences were PCR-amplified using the *nifH*1-4 primers in a nested *nifH* PCR assay (Zani, 1999; Zehr and McCreynolds, 1989) according to details in Cabello et al. (2020). All samples were amplified in duplicate and pooled prior to sequencing. A targeted amplicon sequencing approach was used to create barcoded libraries as described in Green et al. (2015), using 5' common sequence linkers (Moonsamy et al., 2013) on second round primers, *nifH*1 and *nifH*2. Sequence libraries were prepared at the DNA Service Facility at the University of Illinois at Chicago, and multiplexed amplicons were



176 bidirectionally sequenced (2×300 bp) using the Illumina MiSeq platform at the W.M. Keck Center for Comparative and
177 Functional Genomics at the University of Illinois at Urbana-Champaign. Samples were multiplexed to achieve ca. 40,000 high
178 quality paired reads per sample. The AK2HI and NEMO datasets can be found in the SRA (BioProjects PRJNA1062410 and
179 PRJNA1062391, respectively).

180

181 **2.2.3 Sample collection data and co-localized CMAP environmental data**

182 Sample collection data (e.g. coordinates, depth, date) and environmental data provide essential context for the interpretation
183 of diazotroph ‘omics datasets. Large-scale multivariate analyses depend on properly formatted, complete, and ideally quality
184 checked metadata from consistently collected and analyzed measurements. However, accessibility to this information is often
185 limited (especially environmental data) for datasets published across multiple decades. Therefore, we first obtained sample
186 collection metadata from the SRA, and corrected or flagged errors and inconsistencies in the GatherMetadata stage of our post-
187 pipeline workflow (described below), to ensure consistency and completeness. For each sample, the geographic coordinates,
188 depth, and collection date (at local noon) from the SRA were used to query the Simons Collaborative Marine Atlas Project on
189 24 March 2023 (CMAP; <https://simonscmap.com/>; Ashkezari et al., 2021) for co-localized environmental data using a custom
190 script (query_CMAP.py) in the CMAP stage of the workflow (Fig. 1). CMAP is an open-source data portal designed for
191 retrieving, visualizing, and analyzing diverse ocean datasets including research cruise-based and autonomous measurements
192 of biological, chemical, and physical properties, multi-decadal global satellite products, and output from global-scale
193 biogeochemical models. For each sample a mixture of 102 satellite derived and modeled environmental variables from the
194 CMAP repository were obtained. These, along with the SRA collection data, are included in our database. Aggregated metadata
195 for all samples are summarized in Supplementary Table 1 but a detailed description of environmental metadata can be found
196 at the CMAP website (<https://simonscmap.com/catalog>). Metadata are available in the *nifH* ASV database (metaTab.csv for
197 sample metadata and cmapTab.csv for environmental data).

198

199 **2.3 Automated workflow for processing datasets with the DADA2 *nifH* pipeline**

200 **2.3.1 Installation of the DADA2 *nifH* pipeline and the post-pipeline workflow**

201 The workflow (Fig. 1) comprises two software projects installed from separate GitHub repositories, *nifH_amplicons_DADA2*
202 which comprises the ASV pipeline and ancillary scripts, and *nifH-ASV-workflow* which integrates pipeline results for all
203 datasets with annotation and CMAP environmental data to produce the data deliverable of the present work, the *nifH* ASV
204 database. Installation requires cloning the *nifH_amplicons_DADA2* repository
205 (https://github.com/jdmagasin/nifH_amplicons_DADA2; Morando et al., 2024) to a local machine and then downloading
206 several external software packages using miniconda3. Detailed installation instructions are available from the GitHub



207 homepage, as well as a small tutorial to verify the installation on a small *nifH* amplicon dataset and introduce the two main
 208 pipeline commands (`organizeFastqs.R` and `run_DADA2_pipeline.sh`). Altogether the installation and example take 30–40 min.

209 After installing the ASV pipeline, installation of the *nifH*-ASV-workflow proceeds similarly: Clone the GitHub repository
 210 (<https://github.com/jdmagasin/nifH-ASV-workflow>; Morando et al., 2024) and then download a few additional packages with
 211 `miniconda3` (~10 min to complete). For each study, the *nifH*-ASV-workflow includes the pipeline outputs (ASVs and
 212 abundance tables) which were used to create the *nifH* ASV database. Pipeline parameters and FASTQ input tables for each
 213 study are also provided for users who instead wish to rerun the pipeline starting from FASTQs downloaded from the SRA.
 214 Because the *nifH*-ASV-workflow includes data and parameters specific to the studies used in this work, it has a separate
 215 GitHub repository from the pipeline. However, we emphasize that together they comprise the *nifH* amplicon workflow in Fig.
 216 1.
 217

218 Adding a new dataset to the workflow can be summarized in four steps: (1) Start a Unix-like shell that includes the required
 219 software (by “activating” a `miniconda3` environment called `nifH_ASV_workflow`). (2) Generate ASVs for the new dataset by
 220 running it through the pipeline, likely multiple times to tune parameters (Table 2). Output can be placed in the `Data` directory
 221 alongside other studies used in this work, and SRA metadata must be added to `Data/StudyMetadata`. (3) Include the new ASVs
 222 in the workflow by appending rows to the table `GatherASVs/asvs.noChimera.fasta_table.tsv`, which has file paths to all ASV
 223 abundance tables. (4) For each stage shown in Fig. 1, run the associated Makefile or Snakefile from the Unix-like shell by
 224 executing `"make"` or `"snakemake -c1 --use-conda"`, respectively. Documentation resides within each Makefile or Snakefile.
 225 Input tables from the post-pipeline workflow also have embedded documentation.
 226

228 **Table 2. Parameters for controlling the DADA2 *nifH* pipeline.** Default values can be overridden in the text file that is passed to
 229 `run_DADA2_pipeline.sh`. Parameters for "Read trimming" and "Error models" are used in steps 1 and 2 of the pipeline (Fig. 1). The
 230 remaining parameters are important for controlling how DADA2 trims and quality filters the reads, and merges forward and reverse
 231 sequences to create ASVs.

DADA2 <i>nifH</i> pipeline step	Parameter name	Default value	Description	Studies with non-default parameters
Read Trimming with <code>cutadapt</code>	<code>forward</code>	TGYGAYCCN AARGCNGA	Forward primer 5' to 3'. Default is <i>nifH2</i> (Zehr and Mcreynolds, 1989).	None
	<code>reverse</code>	ADNGCCATC ATYTCNCC	Reverse primer 5' to 3'. Default is <i>nifH1</i> (Zehr and Mcreynolds, 1989).	None
	<code>allowMissingPrimers</code>	FALSE	If TRUE, retain read pairs even if primers absent, e.g. if trimmed reads were uploaded to NCBI SRA.	Ding et al., 2021
Error Models	<code>skipNifHErrorModels</code>	FALSE	By default, use only <i>nifH</i> -like reads to train error models. If TRUE, use a random sample of all reads.	None
	<code>NifH_minBits</code>	150	Train error models using reads that align to PFAM00142 at \geq the specified bit score. The trusted cut off in PFAM00142 (25 bits) is always used to	Set to 0 for most studies. Exceptions that used 100 bits were: Bentzon-Tilia et al., 2015; Gradoville et al.,



			filter reads, then <code>NifH_minBits</code> . If set to 0, only the trusted cut off is used.	2020; Shiozaki et al., 2018a; Turk-Kubo et al., 2021.
	<code>NifH_minLen</code>	33	Train error models using reads with ORFs that align with \geq this many residues to PFAM00142.	None
DADA2 filterAndTrim()	<code>id.field</code>	NA	Specify number of ID field if reads do not follow the CASAVA format. Forwarded to <code>filterAndTrim()</code> . If set, usually to 1.	Ding et al., 2021; Wu et al., 2021; Wu et al., 2019; Mulholland et al., 2019; Raes et al., 2020; Tang et al., 2020; Selden et al., 2021; Hallström et al., 2022b; Hallström et al., 2022a
	<code>truncQ</code>	2	Forwarded to <code>filterAndTrim()</code> .	All studies set to 16 unless used <code>truncLen</code> .
	<code>maxEE.fwd</code>	Inf	Forwarded to <code>filterAndTrim()</code> .	All studies set to 2.
	<code>maxEE.rev</code>	Inf	Forwarded to <code>filterAndTrim()</code> .	All studies set to 4.
	<code>minLen</code>	20	Forwarded to <code>filterAndTrim()</code> .	None
	<code>truncLen.fwd</code>	0	Forwarded to <code>filterAndTrim()</code> and <code>truncQ</code> not used.	Gradoville et al., 2020; Sato et al., 2021; Selden et al., 2021; Hallström et al., 2022b
	<code>truncLen.rev</code>	0	Forwarded to <code>filterAndTrim()</code> .	(See <code>truncLen.fwd</code> .)
<code>useOnlyR1Reads</code>	FALSE	If TRUE, only use R1 reads (and do not call <code>mergePairs()</code>). Used if R2 reads are very low quality.	None	
DADA2 mergePairs()	<code>minOverlap</code>	12	Forwarded to <code>mergePairs()</code> .	None
	<code>maxMismatch</code>	0	Forwarded to <code>mergePairs()</code> .	All studies set to 1.
	<code>justConcatenate</code>	FALSE	Forwarded to <code>mergePairs()</code> .	None

232

233

234 2.3.2 DADA2 *nifH* pipeline

235 To encourage reproducible outputs and usage by non-programmers, the DADA2 pipeline (GitHub repository:
 236 `nifH_amplicons_DADA2`) is controlled by a plain text parameters file (Table 2) and a descriptive table of input samples (the
 237 “FASTQ map”). Since a study might include samples with vastly different diazotroph communities and relative abundances,
 238 potentially impacting ASV inferences by DADA2, the FASTQ map for a study enables samples to be partitioned into
 239 “processing groups” that are each run separately through DADA2. For example, in the present work processing groups usually
 240 partitioned the samples in a study by the unique combinations of collection station or date, nucleic acid type (DNA or RNA),
 241 size fraction, and collection depth. Pipeline outputs for each processing group are stored in a directory hierarchy with levels
 242 that follow the processing group definition. Partitioning datasets into processing groups greatly improves the overall speed of
 243 DADA2 and simplifies subsequent analyses that compare ASVs detected in different kinds of samples (e.g., detected versus
 244 transcriptionally active diazotrophs, or presence across different stations, depths, and/or size fractions). For generating the *nifH*
 245 ASV database, studies that met selection criteria (Sect. 2.2.1 and Table 1) were run through the pipeline using the study-
 246 specific FASTQ maps and parameters available in the Data directory of the *nifH*-ASV-workflow GitHub repository.



247

248 The DADA2 pipeline runs from the command line in a Unix-like shell, moving through 9 main steps (Fig. 1 DADA2 *nifH*
249 pipeline): (1) trim reads of primers using cutadapt (Martin, 2011); (2) build sequencing error models; (3) make FASTQ quality
250 plots; (4) trim and filter reads based on quality; (5) dereplicate; (6) denoise (ASV inference); (7) merge forward and reverse
251 sequences; (8) make the ASV abundance table; and (9) remove chimera (Callahan et al., 2016 for steps 2 through 9). These
252 steps will be familiar to DADA2 users, except that for step 2 the error models are trained only on *nifH*-like reads (discussed
253 below). To run the pipeline on other functional genes, the parameters file would need to be edited to disable *nifH*-based error
254 models and to include the expected primers. We again note that the DADA2 pipeline is distinct from the post-pipeline
255 workflow stages which are specific to this work, but together they comprise the workflow in Fig. 1.

256

257 DADA2 parameters impact the ASV sequences identified, and the number of reads used. Thus, exploring parameters is
258 essential for checking the robustness of ASVs (particularly rare ones) and their relative abundances. The DADA2 pipeline
259 supports the optimization of parameters (Table 2). For example, one can trim each read based on its quality degradation (truncQ
260 parameter to the DADA2 filterAndTrim function) or all reads at the same position determined by inspecting FASTQ quality
261 plots. The pipeline allows one to rerun DADA2 steps 3-9, with outputs saved in separate, date-stamped directories. Read
262 trimming and error models (steps 1-2) are unlikely to benefit much from parameter tuning, so the pipeline reuses outputs from
263 those steps. Log files and diagnostic plots created by the pipeline are intended to facilitate parameter evaluation as well to
264 capture statistics to support publication. Moreover, logs and other pipeline outputs are consistently formatted across pipeline
265 runs, which enables scripts to aggregate and analyze results across datasets such as in our workflow.

266

267 Step 1 consisted only of read trimming using cutadapt (Martin, 2011). Raw reads were trimmed and retained only when read
268 pairs for which the forward (*nifH2*) and reverse (*nifH1*) primers were both found on the R1 and R2 reads, respectively. DADA2
269 sequencing error models were built at step 2 using only the reads predicted to be *nifH*, rather than a subsample of all reads as
270 in typical use of DADA2. Reads likely to encode *nifH* were identified as follows: FragGeneScan (version 1.31, (Rho et al.,
271 2010)) was used to predict open reading frames (ORFs) on R1 reads which were then aligned to the nitrogenase PFAM model
272 (PF00142.20) using HMMer3 (hmmsearch version 3.3.2; hmmer.org). ORFs with >33 residues and a bit score that exceeded
273 the trusted cut-off encoded in the model (25.0 bits) were retained. Prefiltering the reads aims to reduce effects of PCR artifacts
274 on the error models. For some studies this approach resulted in increases (~3–10 %) in the total percentage of reads retained
275 in ASVs, and fewer total ASVs, compared to using error models based on a subsample of all reads. Adapting the pipeline to a
276 different marker gene would only require substituting an appropriate PFAM model, or disabling step 2 (by setting
277 skipNifHErrorModels to TRUE; Table 2), which forces the pipeline to make error models by subsampling from all reads. At
278 step 4, DADA2 filterAndTrim() truncated reads at the first base with PHRED score ≤ 16 and discarded read pairs that had
279 excessive errors (>2 for R1 reads, >4 for R2 reads) or were <20 bp. The PHRED quality cut off, which corresponds to a 2.5 %
280 base call error rate, was complemented by conservative parameters for merging sequences: At most 1 base pair was allowed



281 to mismatch in the forward and reverse sequence overlap of minimally 12 bp (stage 7). Dereplicating (step 5) and denoising,
282 ASV calling (step 6), generating an abundance table (step 8), and chimera detection (step 9), were all performed with default
283 DADA2 parameters. Data sets that passed pre-processing steps (Table 1) were run through the DADA2 pipeline using mostly
284 identical parameters (Table 2).

285

286 2.3.3 Post-pipeline stages

287 The workflow post-pipeline stages (GitHub repository: *nifH*-ASV-workflow) combine the pipeline outputs, conduct further
288 quality control steps, co-locate the samples with environmental data from the CMAP data portal, and annotate the ASVs (Fig.
289 1 Post-pipeline stages). Key outputs from the post-pipeline are: a unified FASTA with all the unique ASVs detected across all
290 the studies (i.e. all samples); tables of ASV total counts and relative abundances in all studies; multiple annotations for each
291 ASV by comparison to several *nifH* reference databases; and CMAP environmental data for each sample. These outputs
292 comprise the *nifH* ASV database, and are all available within an R image file (workspace.RData) generated by the workflow
293 which is included in the *nifH*-ASV-workflow repository. Provision as an R image will make the outputs immediately accessible
294 to many researchers who prefer R due to its extensive packages for ecological analysis. The *nifH* ASV database is also available
295 on Figshare (<https://doi.org/10.6084/m9.figshare.23795943.v1>; Morando et al., 2024). The remainder of this section describes
296 each of the post-pipeline stages.

297
298 The GatherAsvs stage aggregated ASV sequences and abundances across all DADA2 pipeline runs (i.e. from all samples and
299 studies). First, ASVs were filtered based on length. Chimera sequences were then removed using UCHIME3 denovo (Edgar,
300 2016) via VSEARCH (Rognes et al., 2016). Chimera sequences were identified within each sample, but the final classification
301 was based on majority vote (chimera or not) across the samples in the processing group. Second, the GatherAsvs stage
302 combined the non-chimeric ASVs from all studies into a single abundance table and FASTA file. Since each study is run
303 independently through the DADA2 pipeline, ASV identifiers are not consistent across studies. Therefore, each unique ASV
304 sequence was renamed with a new unique identifier of the form AUID.*i*, where AUID stands for ASV Universal Identifier.
305 The scripts used to rename the ASVs (assignAUIDs2ASVs.R) and to create the new abundance table
306 (makeAUIDCountTable.R) are available at the *nifH_amplicons_DADA2* GitHub repository (in
307 scripts.ancillary/ASVs_to_AUIDs). The script assignAUIDs2ASVs.R optionally takes an AUID reference FASTA so that
308 AUIDs can be preserved as new datasets are added to future versions of the *nifH* ASV database.

309
310 Both rare and potential non-*nifH* sequences were assessed on the unified AUID tables in the next stage, FilterAuids (Fig. 1).
311 First, possible contaminants were identified by the Makefile invocation of check_nifH_contaminants.sh, provided as an
312 ancillary script in the pipeline GitHub repository. In brief, check_nifH_contaminants.sh first translated all ASVs into amino
313 acid sequences using FragGeneScan (Rho et al., 2010), which were then compared using *blastp* to 26 contaminants known



314 from previous *nifH* amplicon studies (Zehr et al., 2003; Goto et al., 2005; Farnelid et al., 2009; Turk et al., 2011). ASVs that
315 aligned at >96 % amino acid identity to known contaminants were flagged. Next FilterAuids removed samples with ≤ 1000
316 reads, and rare ASVs, defined as those that did not have at least one read in at least two samples or ≥ 1000 reads in one sample.

317
318 Next, the ancillary script, `classifyNifH.sh`, was employed to identify and remove non-*nifH*-like sequences. The script utilized
319 *blastx* to search each ASV against ~ 44 K positive and ~ 15 K negative examples of NifH protein sequences that were found in
320 NCBI GenBank by ARBitrator (run on April 28, 2020; Heller et al., 2014). ASVs were classified based on the relative quality
321 of their best hits in the two databases, similar to the "superiority" check in ARBitrator. An ASV was classified as positive if
322 the E-value of its best positive hit was ≥ 10 times smaller than the E-value for the best negative hit, and vice versa for negative
323 classifications. ASVs failing to meet these criteria were classified as 'uncertain'. The *blastx* searches used the same effective
324 sizes for the two databases (`-dbsize 1000000`), so that E-values could be compared, and retained up to 10 hits (`-max_target_seqs`
325 10).

326
327 The FilterAuids stage of the workflow exclusively discarded ASVs with negative classifications. "Uncertain" ASVs were
328 retained as potential *nifH* sequences not in GenBank. In the last stage, FilterAuids excluded ASVs with lengths that fell outside
329 281–359 nucleotides, a size range which in our experience encompasses the majority of valid *nifH* amplicon sequences
330 generated by nested PCR with *nifH*1–4 primers.

331
332 For each AUID in the *nifH* ASV database, we provide taxonomical annotations using several different approaches,
333 encompassed by the AnnotateAuids stage (Fig. 1) and accessible through ancillary scripts in the GitHub repository (in
334 `scripts.ancillary/Annotation`). The script `blastxGenome879.sh` enables a protein level comparison via *blastx* against a database
335 of 879 sequenced diazotroph genomes ("genome879", <https://www.jzehrlab.com/nifh>). Here, the closest cultivated relative for
336 each AUID was determined by smallest E-value among alignments with ≥ 50 % amino acid identity and ≥ 90 % query sequence
337 coverage. Cautious interpretation is suggested because the reference DB is small and contains only cultivable taxa. Similarly,
338 the top nucleotide match of each AUID was identified by E-value within alignments possessing ≥ 70 % nt identity and ≥ 90 %
339 query sequence coverage obtained by *blastn* against a curated database of *nifH* sequences (July 2017,
340 https://www.zehr.pmc.ucsc.edu/nifH_Database_Public/) by executing the `blastnARB2017.sh` script. Additionally, *nifH* cluster
341 annotations were assigned to each ASV using the classification and regression tree (CART) method of Frank et al. (2016).
342 This approach was implemented as part of a custom tool that predicted ORFs for the ASVs with FragGeneScan, then performed
343 a multiple sequence alignment on the ORFs, and then applied the CART classifier. The tool is available as the ancillary script
344 `assignNifHclustersToNuclSeqs.sh`.

345
346 The Makefile created and searched against two "phylotype" databases, one containing 223 *nifH* sequences from prominent
347 marine diazotrophs including NCDs (Turk-Kubo et al., 2022) and another with 44 UCYN-A *nifH* oligotype sequences (Turk-
348 Kubo et al., 2017). These databases were searched using *blastn* with the effective database size of the ARB2017 database (-



349 dbsize set to ~29 million bases) to enable E-value comparisons across all three searches. For each ASV, we provide phylotype
350 annotations based on the top hit by E-value if the alignment had ≥ 97 % nt identity and covered ≥ 70 % of the ASV. Finally,
351 ORFs for all ASVs were searched for highly conserved residues which are thought to coordinate the 4Fe-4S cluster in NifH,
352 specifically for paired cysteines shortly followed by AMP residues (described in Schlessman et al. 1998). This simple check,
353 performed by the script `check_CCAMP.R`, was intended to complement the reference-based annotations above. Presence of
354 cysteines and AMP could be used to retain ASVs that have no close reference. Absence could be used to flag ASVs that,
355 despite high similarity to a reference sequence, might not represent functional *nifH* (e.g. due to frameshifts).

356
357 Since the annotation scripts provided multiple taxonomic identifications for most of the AUIDs, a primary taxonomic ID was
358 assigned for each AUID using the script `make_primary_taxon_id.py`. If a phylotype annotation (e.g., Gamma A) was assigned,
359 this became the primary taxonomic ID; otherwise, cultivated diazotrophs from genome879 were used (e.g., “*Pseudomonas*
360 *stutzeri*”). Finally, when neither a phylotype nor a cultivated diazotroph could be determined, the *nifH* cluster (e.g. “unknown
361 1G”) was used. AUIDs without an assigned *nifH* cluster or taxonomic rank below domain were removed from the final *nifH*
362 ASV database unless paired cysteines and AMP were detected. This final data filtration step occurred in the WorkspaceStartup
363 stage described below.

364
365 The CMAP stage was managed by a Snakefile that called the script `query_cmap.py` to query the CMAP data portal for co-
366 localized environmental data (Fig. 1). The script was passed the main output from the GatherMetadata stage,
367 `metadata.cmap.tsv`, a table of the collection coordinates, dates at local noon, and depths from all the samples. GatherMetadata
368 reported any samples with missing metadata and ensured standardized formats for the required query fields. Additionally,
369 `query_cmap.py` validated fields prior to querying CMAP. It should be noted that the precision of values obtained from CMAP
370 depend on floating point arithmetic, not the significant digits of the underlying measurement or model. Therefore, prior to an
371 analysis requiring high precision for specific CMAP variables, it is recommended to consult the original producer of the data
372 to determine the significant digits.

373
374 The last stage of the workflow, WorkspaceStartup, filtered out AUIDs that had no annotation and then generated the final *nifH*
375 ASV database, which is comprised of AUID abundance tables (counts and relative), AUID annotations, sample metadata and
376 corresponding environmental data. These data are provided as text files (.csv and FASTA) within a single compressed file
377 (.tgz) that is available in Figshare (<https://doi.org/10.6084/m9.figshare.23795943.v1>; Morando et al., 2024) as well as within
378 the workflow GitHub repository within an R image file (`workspace.RData`).

379 2.4 Diazotroph biogeography from DNA dataset of the *nifH* ASV database

380 The DNA dataset, a custom version of the *nifH* ASV database restricted to DNA samples (representing a majority of the
381 database, only removing 94 samples), was created to showcase the utility of the workflow. Additional data reduction steps

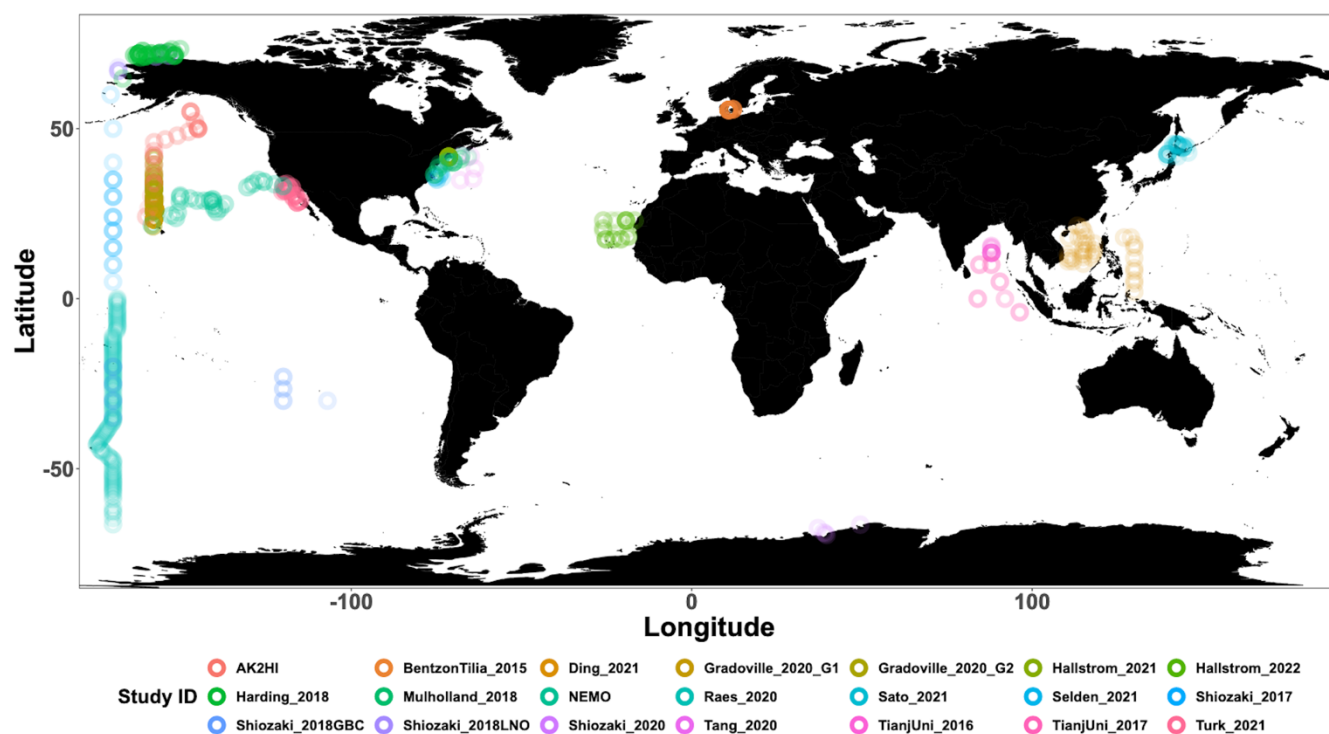


382 were conducted, averaging replicates and samples from the same location but different size fractions, to enable comparisons
383 between different sampling methodologies.

384 3 Results and Discussion

385 3.1 Generation of the marine *nifH* ASV database

386 All publicly available marine *nifH* amplicon HTS data from studies that met our criteria, including two new studies, were
387 compiled in the present investigation (see Sect. 2.2 and Table A1). Altogether 982 samples from 21 studies, comprising a total
388 of 87.7 million reads (Table 3), were processed through the entire workflow, i.e., the DADA2 *nifH* pipeline (Sect. 2.2.2) as
389 well as the post-pipeline stages (Sect. 2.2.3). The *nifH* ASV database, i.e., the ASV sequences, abundances, and annotations,
390 as well as sample collection and CMAP environmental data, was generated from the 865 samples, 7909 ASVs, and 34.4 million
391 reads that were retained by this workflow (Figs. 1 and 2 and Table 3). To our knowledge it is the only global database for
392 marine diazotrophs detected using *nifH* HTS amplicon sequencing, with comprehensive, standardized ancillary data (Fig. 2
393 and Supplementary Table 1).



396
397
398

Figure 2: Global sampling distribution of the *nifH* ASV database. World map of sampling locations for the datasets compiled and processed to construct the *nifH* ASV database. See Table 1 for the citation source linked to each study ID.



399
400
401
402
403

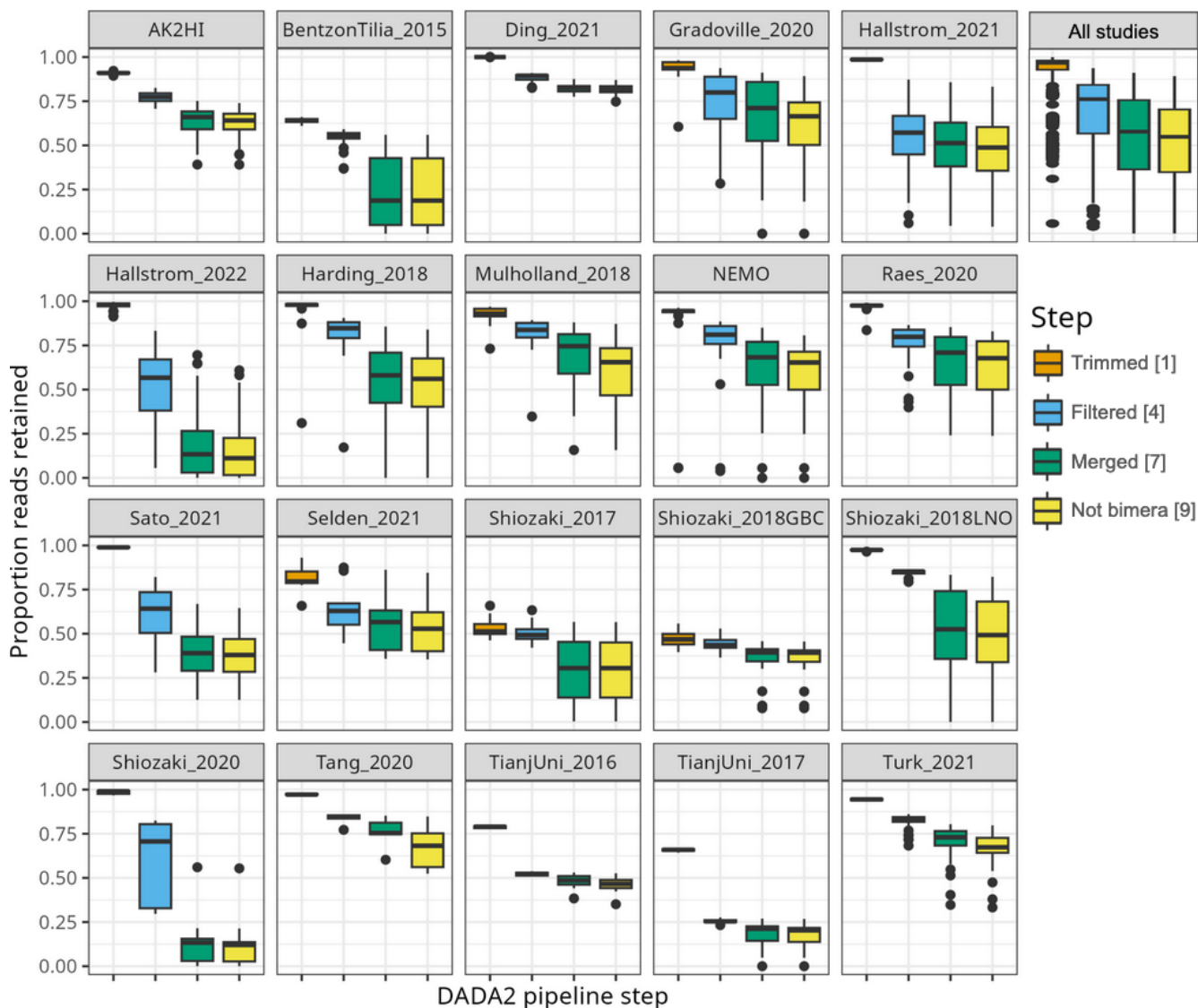
404
405
406
407
408
409

410
411
412
413

Table 3: Summary of the full *nifH* workflow. The number of samples, ASVs, and reads retained through the entire workflow (the DADA2 *nifH* pipeline and major post-pipeline stages) to create the *nifH* ASV database. The vast majority ASVs that were removed by GatherAsvs fell outside 200–450 nt. WorkspaceStartup removed ASVs with no annotation and samples that had zero reads after ASV filtering.

	Initial	DADA2 pipeline	Gather Asvs	FilterAuids				Workspace Startup
				<1K reads in sample	rare	non-NifH	length	
Samples	982	982	982	894	890	890	890	865
ASVs	n/a	177,935	97,205	97,172	13,774	12,479	9,416	7,909
Reads (millions)	87.7	43.3	38.7	38.6	36.4	36.0	35.1	34.4

Interestingly, studies were affected differently by each step of the DADA2 *nifH* pipeline (Fig. 3 and Table 4). There were major losses of reads during ASV merging, with several studies retaining <25 % of their total reads by the end of the pipeline (i.e., BentzonTilia_2015, Hallstrom_2022, Shiozaki_2020, and TianjUni_2016), though on average about half the reads were retained across studies (Fig. 3 and Table 4).



414

415
 416
 417
 418

Figure 3: Study-specific retention of reads at each stage of the pipeline. The proportion of total reads in each sample that are retained at the completion of each step of the DADA2 *nifH* pipeline. Each box shows the distribution for samples in the indicated study (using Study IDs in Table 1), or for all samples together (top right). Proportions for Shiozaki_2017 and Shiozaki_2018GBC reflect that approximately half the amplicons were not in the orientation expected by the pipeline (see text). Numbers in the legend indicate pipeline steps in Fig. 1.

419
 420
 421
 422
 423

Table 4: Quality filtering by the DADA2 *nifH* pipeline. For each study ID are shown the mean numbers of reads retained per sample at the end of each stage of the DADA2 *nifH* pipeline, as well as the mean percentage of reads retained. Statistics in the bottom three rows pool all samples. Initial, Trimmed⁴, Filtered⁴, and Merged⁷ and non-Bimera⁹ and their superscripts are specific to the pipeline steps in Fig. 1. At each step (column) the calculations include only the samples that have >0 reads.

Study	Initial	Trimmed ⁴	Filtered ⁴	Merged ⁹	Non-bimera ⁹	Retained (%)
-------	---------	----------------------	-----------------------	---------------------	-------------------------	--------------



AK2HI	4.5E+04	4.1E+04	3.5E+04	2.8E+04	2.8E+04	62	
BentzonTilia_2015	8.2E+03	5.3E+03	4.6E+03	2.2E+03	2.1E+03	26	
Ding_2021	5.6E+04	5.6E+04	4.8E+04	4.5E+04	4.5E+04	82	
Gradoville_2020	4.0E+04	3.8E+04	2.9E+04	2.6E+04	2.4E+04	61	
Hallstrom_2021	2.5E+05	2.5E+05	1.5E+05	1.4E+05	1.4E+05	49	
Hallstrom_2022	2.0E+05	1.9E+05	1.0E+05	5.4E+04	4.6E+04	19	
Harding_2018	4.2E+04	4.1E+04	3.5E+04	2.4E+04	2.3E+04	54	
Mulholland_2018	1.8E+05	1.6E+05	1.5E+05	1.2E+05	1.1E+05	61	
NEMO	5.7E+04	5.4E+04	4.6E+04	3.7E+04	3.5E+04	60	
Raes_2020	9.3E+04	9.1E+04	7.4E+04	6.6E+04	6.3E+04	63	
Sato_2021	7.5E+04	7.4E+04	4.5E+04	2.9E+04	2.9E+04	39	
Selden_2021	1.5E+05	1.2E+05	9.2E+04	8.2E+04	8.0E+04	55	
Shiozaki_2017	1.8E+04	9.3E+03	8.9E+03	5.8E+03	5.8E+03	28	
Shiozaki_2018GBC	2.4E+04	1.1E+04	1.1E+04	9.2E+03	9.1E+03	35	
Shiozaki_2018LNO	6.7E+04	6.5E+04	5.6E+04	3.5E+04	3.3E+04	49	
Shiozaki_2020	2.5E+05	2.5E+05	1.9E+05	3.4E+04	3.3E+04	12	
Tang_2020	4.7E+04	4.6E+04	3.9E+04	3.5E+04	3.2E+04	67	
TianjUni_2016	8.0E+04	6.3E+04	4.2E+04	3.9E+04	3.7E+04	46	
TianjUni_2017	8.0E+04	5.3E+04	2.0E+04	1.5E+04	1.4E+04	18	
Turk_2021	5.5E+04	5.2E+04	4.6E+04	4.0E+04	3.7E+04	66	
All samples and studies	mean	8.9E+04	8.5E+04	6.1E+04	4.8E+04	4.5E+04	52
	median	5.1E+04	4.8E+04	3.8E+04	2.9E+04	2.8E+04	56
	sum	8.8E+07	8.4E+07	5.9E+07	4.6E+07	4.3E+07	49

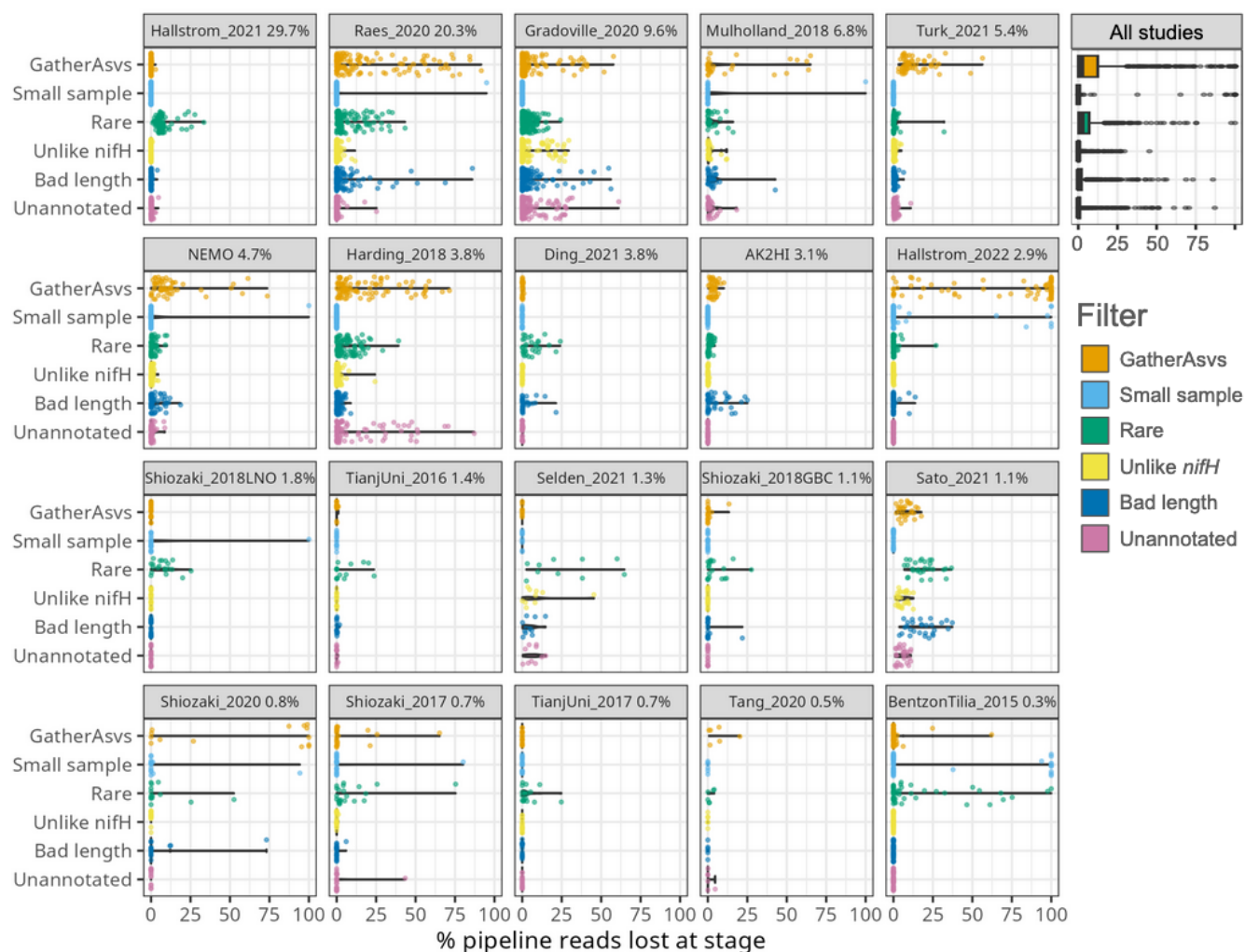
424
 425
 426
 427
 428
 429
 430
 431

Switching the trimming approach from one based on individual read quality profiles (using truncQ in Table 3) to fixed-length trimming based on overall quality profiles of the forward and reverse reads (using truncLen.fwd and truncLen.rev in Table 2) resulted in more reads being retained for some studies (Sato et al., 2021; Selden et al., 2021; Hallström et al., 2022b; Gradoville et al., 2020). However, fixed-length trimming would have required the selection of trim lengths based on visual, qualitative assessments of hundreds of FASTQ quality plots which is difficult to accomplish in a systematic manner. For consistency we preferred to use nearly identical parameters for most studies (Table 3).



432
 433
 434
 435
 436
 437
 438
 439
 440
 441

Post-pipeline stages of the workflow further refined the data (detailed in Methods) (Fig. 4). First, GatherAsvs identified and removed 112 chimeras using uchime3 denovo (distinct from the bimera filtering done by the pipeline), and then removed 81 K ASVs that were far outside expected *nifH* lengths (200–450 nt). AUIDs were assigned to the remaining 97 K unique non-chimeric ASVs (comprising 38.7 million total reads; Tables 3 and 5). The GatherAsvs length filter had by far the largest impact of any post-pipeline quality filtering, removing 10 % of the reads from the pipeline. Next, FilterAuids dropped four poorly sequenced samples (7 K total reads), as they would likely misrepresent their diazotrophic communities, and then removed 83 K rare ASVs (2.3 million reads; Tables 3 and 5).



442
 443



444 **Figure 4: Study-specific retention of reads at each stage of the post-pipeline workflow.** For each study the violin plots show how many
 445 reads from the pipeline were removed by GatherAsvs due to length, the four filtering steps of FilterAuids, or WorkspaceStartup due to the
 446 ASV having no annotation (shown in Fig. 1). Losses for all samples combined are shown in the box plot (top right). Studies are ordered by
 447 contribution to the *nifH* ASV database, e.g. 29.7 % of all the reads in the database were from Hallstrom_2021.

448
 449

450 **Table 5. Quality filtering by the post-pipeline workflow.** For each study are shown the mean numbers of reads per sample that were output
 451 by the DADA2 *nifH* pipeline and retained by the GatherAsvs, FilterAuids, and WorkspaceStartup stages of the post-pipeline workflow. The
 452 Retained (%) column has the mean percentages of reads retained per sample (relative to column DADA2 pipeline values). Additionally, the
 453 last three rows show the overall means, medians, and sums of reads across all samples and studies. Superscripts correspond to stage numbers
 454 in Fig. 1 Post-pipeline stages. The GatherAsvs¹ column mainly reflects length filtering (200–450 nt), and the WorkspaceStartup⁶ column
 455 reflects discarding of ASVs that had no annotation. At each stage (column) the calculations include only the samples that have >0 reads.

456

Study ID	DADA2 pipeline	Gather Asvs ¹	FilterAuids ²			Workspace Startup ⁶	Retained (%)
			Rare	Non-NifH	Length		
AK2HI	2.8E+04	2.7E+04	2.7E+04	2.7E+04	2.5E+04	2.5E+04	90
BentzonTilia_2015	2.1E+03	2.1E+03	2.6E+03	2.6E+03	2.6E+03	2.6E+03	85
Ding_2021	4.5E+04	4.5E+04	4.2E+04	4.2E+04	4.1E+04	4.1E+04	91
Gradoville_2020	2.4E+04	2.3E+04	2.2E+04	2.1E+04	2.1E+04	2.0E+04	80
Hallstrom_2021	1.4E+05	1.4E+05	1.3E+05	1.3E+05	1.2E+05	1.2E+05	92
Hallstrom_2022	4.6E+04	2.6E+04	3.8E+04	3.8E+04	3.4E+04	3.4E+04	50
Harding_2018	2.3E+04	1.9E+04	1.8E+04	1.7E+04	1.7E+04	1.5E+04	64
Mulholland_2018	1.1E+05	9.3E+04	9.3E+04	9.1E+04	8.7E+04	8.4E+04	72
NEMO	3.5E+04	3.1E+04	3.1E+04	3.1E+04	3.0E+04	3.0E+04	80
Raes_2020	6.3E+04	5.8E+04	5.6E+04	5.6E+04	5.6E+04	6.0E+04	76
Sato_2021	2.9E+04	2.7E+04	2.1E+04	2.0E+04	1.5E+04	1.4E+04	43
Selden_2021	8.0E+04	8.0E+04	6.0E+04	5.2E+04	4.9E+04	4.4E+04	52
Shiozaki_2017	1.2E+04	1.2E+04	1.1E+04	1.1E+04	1.1E+04	1.1E+04	83
Shiozaki_2018GBC	2.0E+04	2.0E+04	2.0E+04	2.0E+04	2.0E+04	2.0E+04	93
Shiozaki_2018LNO	3.3E+04	3.3E+04	3.3E+04	3.3E+04	3.3E+04	3.3E+04	92
Shiozaki_2020	3.3E+04	2.8E+04	4.2E+04	4.2E+04	5.7E+04	5.7E+04	61
Tang_2020	3.2E+04	3.0E+04	2.9E+04	2.9E+04	2.9E+04	2.9E+04	91
TianjUni_2016	3.7E+04	3.7E+04	3.5E+04	3.5E+04	3.5E+04	3.5E+04	93
TianjUni_2017	1.4E+04	1.4E+04	1.4E+04	1.4E+04	1.4E+04	1.4E+04	96
Turk_2021	3.7E+04	3.3E+04	3.3E+04	3.2E+04	3.2E+04	3.2E+04	83



All samples and studies	mean	4.5E+04	4.2E+04	4.1E+04	4.0E+04	4.0E+04	4.0E+04	79
	median	2.8E+04	2.6E+04	2.6E+04	2.6E+04	2.5E+04	2.6E+04	90
	sum	4.3E+07	3.9E+07	3.6E+07	3.6E+07	3.5E+07	3.4E+07	79

457

458

459

460

461

462

463

464

465

466

467

468

Finally, ASVs were removed if they were classified as non-*nifH*, based on a strong alignment to sequences in NCBI nr that ARBitrator (Heller et al., 2014) classified as non-*nifH*. Specifically, an ASV was classified as non-*nifH* if the ratio of E-values for its best negative and positive hits, among sequences classified by ARBitrator, was >10 . A total of 96,095 of the 97,205 non-chimera ASVs had database hits which resulted in 40,448 positive, 12,977 negative, and 42,670 uncertain classifications. This approach was used to leverage ARBitrator's high specificity for detecting *nifH* as well as to enable users to identify ASVs that have high percent identity matches to sequences in GenBank. An alternative approach would have been to classify the ASVs based on their alignments to HMMs for NifH versus NifH-like proteins (e.g. protochlorophyllide reductase), used by the NifMAP pipeline for *nifH* operational taxonomic units (Angel et al., 2018). Finally, FilterAuids removed ASVs with lengths outside 281–359 nt, a total of 974 K reads and 3063 ASVs (Figs. 1, 4 and Tables 3 and 5). After FilterAUIDs, the total number of samples in the dataset was reduced from 982 to 890 and the number of ASVs from 97,205 to 9416.

469

470

471

472

473

474

FilterAuids also flagged a total of 2000 ASVs as possible PCR contaminants. Although we opted to flag, not remove, these ASVs, the workflow can be easily altered to remove contaminants. Most studies contained low levels of contamination ($\leq 1\%$) based on our criteria. However, several studies were flagged with $\sim 9\text{--}30\%$ of their reads being similar to known contaminants. Identifying potential contaminants is challenging given their numerous sources, study specific nature (Zehr et al., 2003), and lack of control sequence data from blanks.

475

476

477

478

479

480

481

482

483

484

485

Next, AnnotateAuids assigned annotations using our three *nifH* reference databases and CART (Fig. 1). In total 7931 of the 9416 quality filtered ASVs were annotated, usually with multiple references (Fig. A1). Most (7926 ASVs) had hits to both genome879 and ARB2017, likely because the 879 sequenced diazotrophs had *nifH* homologs in GenBank that were found by ARBitrator. Fewer ASVs had hits to the databases that targeted UCYN-A oligos (102 ASVs) and other marine diazotrophs (645 ASVs; 96 ASVs also had UCYN-A hits). Most ASVs (7905 total) were assigned to NifH clusters 1–4 by CART (respectively, 4100; 79; 3607; and 109 ASVs), including five ASVs that had no hits to our databases. The majority of ASVs (7749 total) had open reading frames (ORFs) that contained paired cysteines and AMP which might coordinate the 4Fe-4S cluster, and all 7749 also had annotations from the reference databases or CART. A few ASVs had annotations but lacked residues to coordinate 4Fe-4S: 23 ORFs lacked the paired cysteines and another 159 ORFs had paired cysteines but not AMP, usually due to a substitution for M. The last step of AnnotateAuids assigned primary IDs (described above) to 7908 ASVs. In the final stage of the post-pipeline workflow, WorkspaceStartup retained these 7908 ASVs. One ASV, which had no



486 phylogroup but did have paired cysteines and AMP, was also retained. In total the *nifH* ASV database had 7909 ASVs
487 comprising 34.4 million reads (Table 3).

488
489 In the CMAP stage, sample collection metadata (date, latitude, longitude, and depth) were used to download CMAP
490 environmental data (102 variables) for each sample in the *nifH* ASV database (Fig. 1). The CMAP data will enable analyses
491 of potential factors that influence the global distribution of the diazotrophic community. Aggregated metadata for all samples
492 are available in the *nifH* ASV database (metaTab.csv for sample metadata and cmapTab.csv for environmental data).

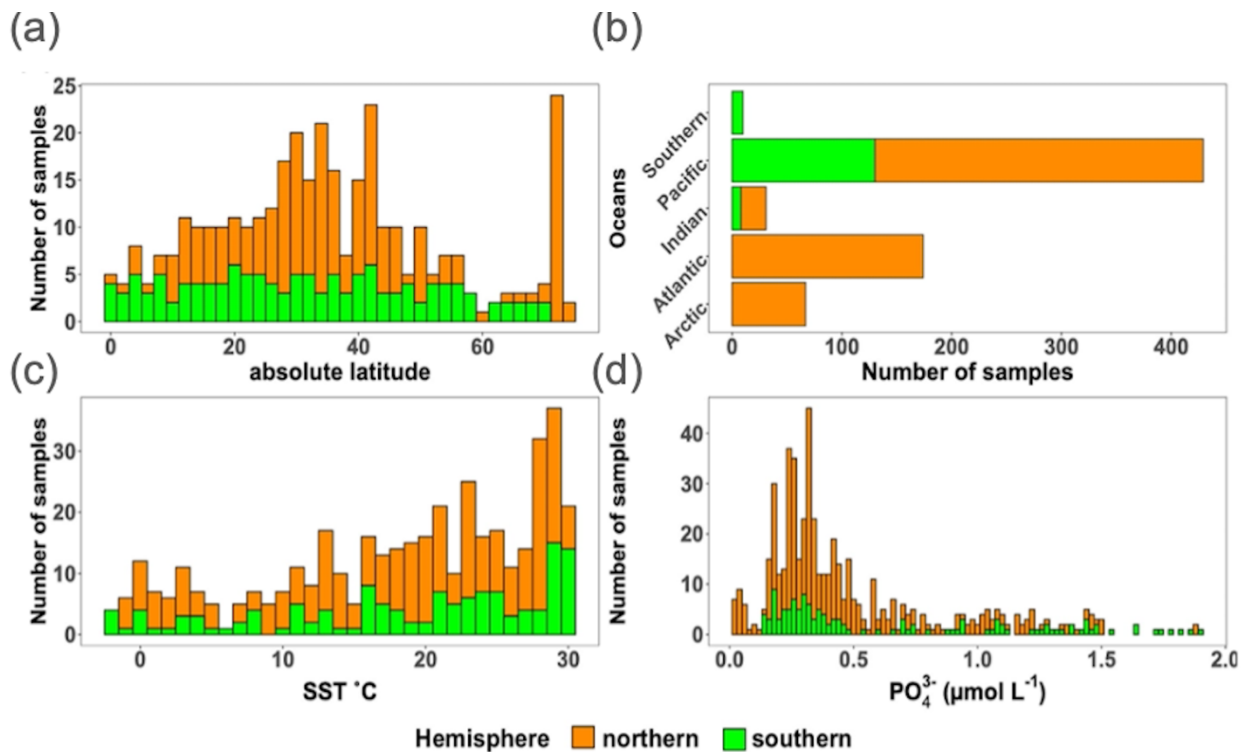
493
494 The last stage of the post-pipeline workflow is WorkspaceStartup, which generates the *nifH* ASV database (Fig. 1). ASVs with
495 no annotation are removed as well as samples with zero total reads due to ASV filtering steps. The *nifH* ASV database consisted
496 of 21 studies, 865 samples, 7909 AVS and 34.4 million total reads (Tables 3 and 5). The database is heavily biased toward
497 euphotic zone DNA samples, with euphotic heuristically defined as follows: Samples were classified as coastal (< 200 km
498 from a major landmass) or open ocean. Euphotic samples were then identified as those collected above a depth cut off, 50 m
499 for coastal samples and 100 m for open ocean. Samples obtained from DNA (n=768) far exceeded those from RNA (n=94)
500 extracts. Likewise, a majority of the samples were from the euphotic zone (789 compared to 73 from the aphotic zone). The
501 database also includes replicate samples (n=256) and size fractionated samples (n=142).

502 **3.2 Global *nifH* ASV database**

503 **3.2.1. Sample Distribution**

504 Investigations of N₂ fixation and diazotrophic communities have focused on specific ocean regions and this is reflected by the
505 uneven global distribution of *nifH* amplicon datasets in the *nifH* ASV database (Figs. 2, 5a, and 5b). There is an outsized
506 influence of the northern hemisphere, especially in the Pacific Ocean where most of the database samples were located (429)
507 and 69.7 % of these samples originated from the northern hemisphere (Figs. 2, 5a, 5b, and 6). Ten studies are found within the
508 Pacific, with several containing >50 samples (Figs. 2 and 6). Notably, Raes_2020 (Raes et al., 2020) is the largest dataset
509 stretching from the equator to the Southern Ocean, making up almost the entirety of the southern hemisphere Pacific samples
510 (Figs. 2 and 6). Two new studies carried out in the North Pacific constitute the only previously unpublished data of the *nifH*
511 ASV database (Table 1). AK2HI was a latitudinal transect from Alaska (U.S.) to Hawaii (U.S.) and NEMO was a longitudinal
512 transect across the Eastern North Pacific from San Diego, CA (U.S.) to Hawaii (U.S.) (Fig. 2; Sect. 2.2.2). The amplicon data
513 compiled for the *nifH* ASV database was primarily generated from DNA, with most RNA samples deriving from Atlantic
514 Ocean studies and no contribution from RNA samples in the Arctic or Indian Oceans (Fig. 6).

515
516



517
518

519
520
521

Figure 5. Location, temperature, and phosphate distributions of the *nifH* ASV database. The number of samples from the *nifH* ASV database by (a) absolute latitude, (b) the world's oceans, (c) sea surface temperature (SST, °C) and (d) Pisces-derived PO₄³⁻ (μmol L⁻¹). Environmental data, (c) and (d), were retrieved from the CMAP data portal.

522
523
524

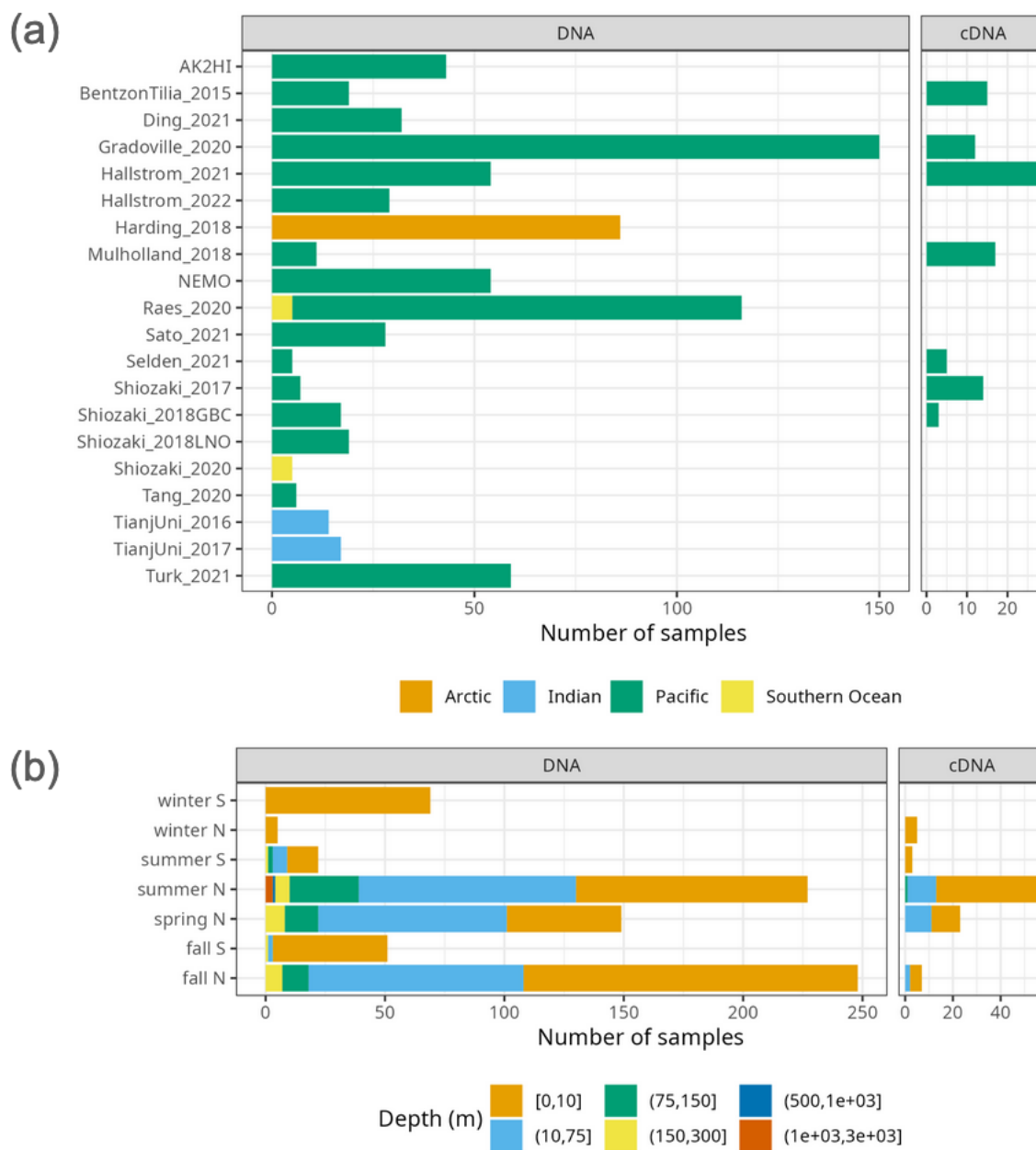


Figure 6. Samples in the *nifH* ASV database by collection location, season, and amplicon type. The number of samples from each study are shown by ocean and study (a), and by the collection season, hemisphere, and depth (b). For both panels the amplicon type (DNA or cDNA) is shown, but x axis scales differ between (a) and (b). See Table 1 for citations for the studies in (a). For (b) there were no samples collected between 500–1000 m.

525
 526
 527
 528
 529
 530

531
 532



533 Under-sampled regions include the Eastern South Pacific (n=6) and the Western Indian Ocean (n=0) (Figs. 2, 5a, and 6a). Only
534 two studies originated from the Indian Ocean, a unique environment with intense weather and shifting circulation patterns that
535 include monsoon seasons and upwelling conditions that will require much greater sampling coverage to capture diazotroph
536 biogeography. No South Atlantic samples were found during compilation that met the criteria for inclusion in the *nifH* ASV
537 database, though there are several studies from this region (Table A1). Most Atlantic Ocean samples were coastal and from
538 the North Atlantic. Thus, the Atlantic subtropical gyres, which are known to host diverse diazotrophs (Langlois et al., 2005),
539 are underrepresented by *nifH* amplicon data (Fig. 2).

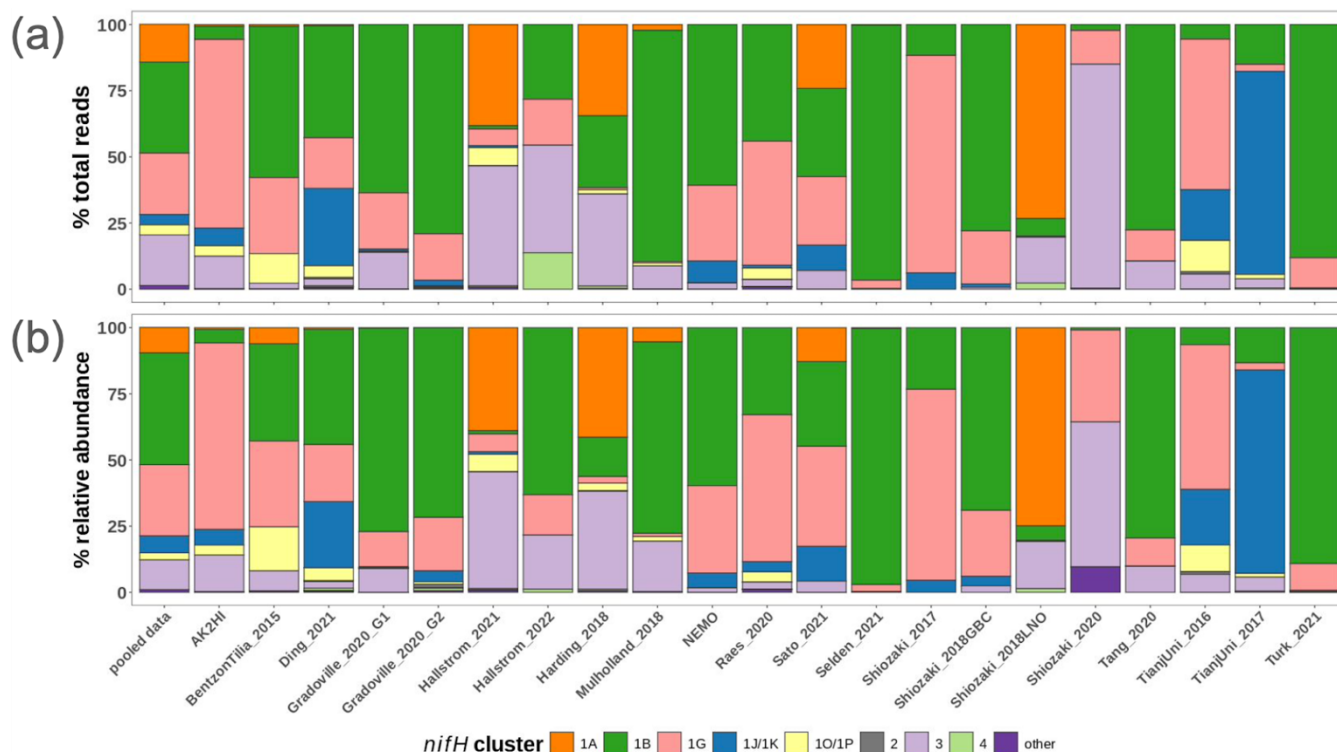
540
541 Tropical and subtropical regions, often associated with high temperatures and low nutrients, are highly represented in the
542 database (Figs. 2 and 5a). This likely influenced the ranges of environmental variables with most samples in the database
543 originating from locations with SST above 15 °C and PO₄³⁻ below 0.5 μmol L⁻¹ (Figs. 5c and 5d). Northern hemisphere samples
544 were collected in all seasons, though fewer from the winter. In contrast, most southern hemisphere samples were collected in
545 the winter and fall (Fig. 6b). While most DNA samples are from the euphotic zone (Fig. 6b), cDNA samples are almost
546 exclusively from the euphotic zone, and mainly from the northern hemisphere during the spring and summer (Fig. 6b),
547 indicating an incomplete picture of diazotroph activity.

548
549 The disproportionate spatial and seasonal coverage between hemispheres in the *nifH* ASV database mirrors collection biases
550 in other N₂ fixation metrics including: N₂ fixation rate measurements; diazotroph cell counts; and *nifH* qPCR data, which are
551 heavily sourced from the North Atlantic (Shao et al., 2023) or, when targeting NCDs, also the North Pacific (Turk-Kubo et al.,
552 2022). These biases underscore the need for future work in understudied regions and seasons.

553 3.3 Study-specific patterns in global diazotroph assemblages in the DNA dataset

554 To demonstrate how the *nifH* ASV database can be used, a subset of the data was created that comprised of all DNA samples
555 (89.1 % of the total dataset; Fig. 7) and referred to herein as the “DNA dataset”. Samples derived from cDNA (n=94; Fig. 6)
556 were removed. Replicate samples (n=256) or those with multiple size fractions (n=142) were combined by averaging across
557 replicates or size fractions. This reduced the number of DNA samples to 711 and the total number of reads in the count table
558 to 30.0 million from 34.4 million.

559
560
561
562



563

564

565

566

567

568

569

570

571

572

573

574

575

576

577

578

579

580

581

582

Figure 7. Study-specific diazotroph assemblage patterns in the DNA dataset. The percentage of (a) total reads and (b) relative abundance over the DNA dataset for each major *nifH* cluster. The first column of each panel ('pooled data') uses all the compiled data while each subsequent column only uses data from the indicated study. Colors represent different *nifH* subclusters; 'other' are the remaining *nifH* clusters.

As demonstrated in a previous global analysis of diazotroph assemblages (Farnelid et al., 2011), cyanobacterial sequences (cluster 1B) dominate the samples, making up 34 % and 42 % of the total reads and relative abundance, respectively (Fig. 7). Though photosynthetic cyanobacteria would be expected to thrive in euphotic waters, NCDs are also widespread in the ocean surface (Langlois et al., 2005; Delmont et al., 2018; Delmont et al., 2022; Pierella Karlusich et al., 2021; Turk-Kubo et al., 2022). Indeed, among the NCDs, γ -proteobacteria (*nifH* cluster 1G) were the most prevalent, comprising ca. 23 % of total reads and 27 % of relative abundance, while δ -proteobacteria (clusters 1A and 3) accounted for 33 % of total reads and 21 % of relative abundance of the DNA dataset (Fig. 7). Less prominent clusters 1J/1K (α - and β -proteobacteria) and 1O/1P (γ -/ β -proteobacteria and Deferribacteres) were ca. 4 % and 6 % of the reads and 4 % and 3 % of the relative abundance, respectively. The remaining ASVs comprised <1.5 % of the total reads and relative abundances and came from clusters associated with nitrogenases that do not use iron (e.g. cluster 2) or that are uncharacterized (cluster 4) (Fig. 7).

Cluster 1B (cyanobacteria) were generally high in individual studies across the *nifH* DNA dataset, comprising ≥ 25 % of the relative abundance community in two-thirds of the studies (Fig. 7), which is the highest of any cluster. Studies carried out in



583 polar regions (Harding_2018, Shiozaki_2018LNO, Shiozaki_2020) and the Indian Ocean (TianjUni_2016 and TianjUni_2017)
584 were distinct from this pattern, with low relative abundances of cluster 1B. Instead, Arctic studies had high relative abundances
585 of cluster 1A and 3 (both primarily comprised of δ -proteobacteria) and while clusters 1J/1K (α - and β -proteobacteria) and
586 1O/1P (γ -/ β -proteobacteria and Deferribacteres) were the predominate groups in the Indian Ocean.

587
588 The second most abundant group was the cluster 1G (γ -proteobacteria), making up ca. 25 % of the total reads across the DNA
589 dataset, with study-specific relative abundances greater than 25 % in eight out of 21 studies (Fig. 7). Members of this group
590 were often found at high relative abundances in Pacific Ocean studies (AK2HI, NEMO, Raes_2020, Sato_2021,
591 Shiozaki_2017), as well as in other ocean regions including the Atlantic (BentzonTilla_2015), Indian (TianjUni_2016) and
592 Southern Ocean (Shiozaki_2020). The notable exception is in Arctic studies, where cluster 1G was almost absent (Fig. 7).

593
594 In several studies, including BentzonTilla_2015, Hallstrom_2021, Mulholland_2018, Selden_2021, Tang_2020, and
595 Hallstrom_2022, diazotroph assemblages had high relative abundances of putative δ -proteobacteria (clusters 1A and 3),
596 reflecting possibly a coastal/shelf or upwelling signature (Figs. 2 and 7). The only study with samples primarily from the
597 Southern Ocean (Shiozaki_2020) was also the only study with a large portion of *nifH* cluster 1E (*Bacillota*).

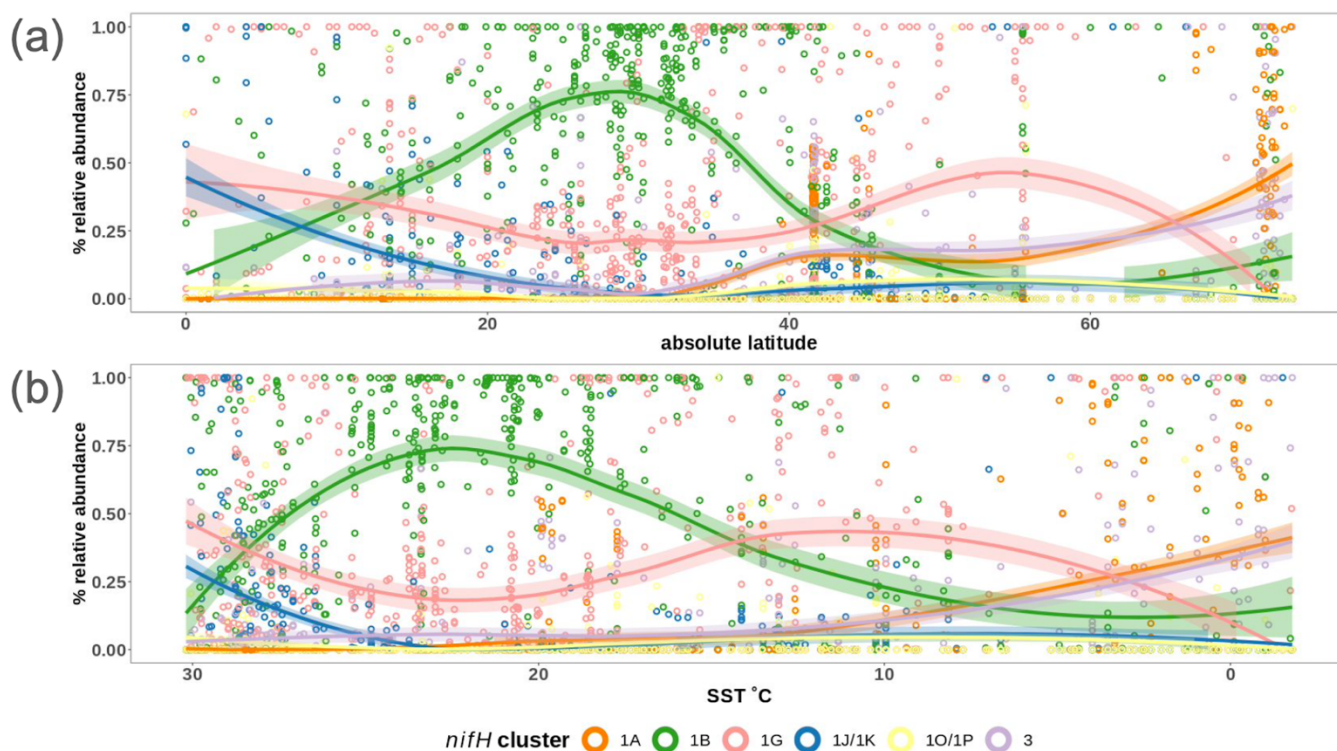
598 3.3.2 Emerging patterns in global diazotroph assemblages across the DNA dataset

599 The *nifH* ASV database enables new analyses of global diazotroph biogeography in the context of environmental parameters,
600 through co-localization with satellite and model outputs publicly available through CMAP (Ashkezari et al., 2021). To
601 demonstrate the utility of the *nifH* ASV database, we present here patterns in relative abundances of *nifH* clusters across
602 absolute latitude and SST in the DNA dataset. Cosmopolitan distributions were evident for γ -proteobacterial (1G) and
603 cyanobacterial diazotrophs (1B; Fig. 8a), corroborating and extending previous findings (Farnelid et al., 2011; Shao and Luo,
604 2022; Halm et al., 2012; Fernandez et al., 2011; Löscher et al., 2014; Cheung et al., 2016). At low to mid latitudes, γ -
605 proteobacterial (1G) diazotrophs generally had high relative abundances and were often the dominant taxa when present.
606 However, they declined within the gyre regions, ranging between ~25–50 % of the population when present, while
607 cyanobacterial diazotrophs (1B) increased and became dominant in the subtropical gyres (Fig. 8a). Notably, cluster 1G
608 diazotrophs reached high relative abundances in each transitional zone, before mainly disappearing at latitudes above 56° (Fig.
609 8a). However, as mentioned previously, sampling bias likely plays a large role at these higher latitudes where the number of
610 studies and samples are sparse (Figs. 2 and 5).

611
612 Clusters 1B and 1G were both detected over the full range of SST (approximately -2–30 °C) but peaks in their relative
613 abundances occurred in distinct SST ranges. Cyanobacterial diazotrophs had multiple peaks in relative abundance in waters
614 >18 °C underscoring their dominance in tropical gyre regions (Fig. 8b). The 1G cluster also spanned the entire temperature



615 spectrum but had notably higher presence and relative abundance above SSTs of 8 °C and 11 °C, respectively (Fig. 8b). The
616 overlap between 1G and 1B has been reported previously, however the factors controlling this are unknown (Moisander et al.,
617 2014; Shiozaki et al., 2017; Shiozaki et al., 2018b; Liu et al., 2020; Tang et al., 2020; Messer et al., 2015).
618
619



620
621 **Figure 8: Global distribution of major *nifH* clusters in the DNA dataset.** The relative abundance of *nifH* genes for each major *nifH*
622 cluster from every sample compiled in the DNA dataset versus (a) absolute latitudinal and (b) SST. Smoothing averages (lines) were
623 calculated using local polynomial regression fitting (LOESS) with 95% confidence intervals (translucent colored areas). Each color
624 represents a different *nifH* cluster. SST in (b) is from warmest to coolest temperatures to show that trends are similar to those in (a).

625
626 δ -proteobacterial diazotrophs (clusters 1A and 3) were generally found in cooler, higher latitude waters. Notably, both clusters
627 1A and 3 were mainly found below ~10°C (Fig. 8b). δ -proteobacteria associated with cluster 1A were generally found at
628 latitudes >32° and reached maximum relative abundances near the poles, including in the Beaufort Sea, the highest latitude
629 region surveyed (72°; Figs. 2, 5, and 8a). The vast majority of cluster 1A δ -proteobacteria were found at SST ≤5 °C (Fig. 8b).
630 Though cluster 3 and 1A distributions were similar, cluster 3 showed broader spatial and temperature ranges, with consistent
631 but low relative abundances in the subtropics and tropics (Fig. 8).
632



633 In contrast, the relative abundances of cluster 1J/1K and 1O/1P diazotrophs declined as SST decreased and latitude increased,
634 becoming rare at higher latitudes (Fig 8). The highest relative abundances for these clusters were observed near the equator,
635 and in some cases, comprised 100% of the diazotroph assemblage in high SST, tropical samples. These patterns suggest that
636 temperature was an important factor controlling the narrow SST band (≥ 26 °C) clusters 1J/1K and 1O/1P occupied, establishing
637 them as the *nifH* clusters with the smallest geographic range in the *nifH* ASV database (Fig. 8).
638
639

640 3.4 Limits and caveats to interpreting *nifH* amplicon data

641 The PCR amplification of the *nifH* gene and its transcripts has been vital in advancing the knowledge of diazotroph ecology
642 due to its high sensitivity, detecting diazotrophs at abundances that are often orders of magnitude lower than other marine
643 microbes. This approach has facilitated the discovery of many novel diazotrophs, and provided the first evidence of the
644 widespread distribution of unicellular diazotrophs throughout the open oceans (Falcon et al., 2004; Falcon et al., 2002; Zehr
645 et al., 1998; Zehr et al., 2001). Advances in HTS technologies have revealed diverse diazotrophic assemblages, including the
646 ubiquitously distributed NCDs (Turk-Kubo et al., 2014; Shiozaki et al., 2017; Raes et al., 2020). These discoveries have
647 fostered a new perspective of global diazotrophic ecology (Zehr and Capone, 2020), improved our models of diazotrophic
648 distributions and global N fixation rates (Tang et al., 2019) and will continue to drive new research questions.
649

650 However, interpreting *nifH* PCR-based data requires the consideration of several important caveats. Diazotrophs constitute a
651 small fraction of the total microbial community, and thus often require numerous PCR cycles in conjunction with nested PCR
652 for detection. Increasing the number of cycles can exacerbate known amplification biases (Turk et al., 2011) and increase the
653 likelihood of detecting contaminant sequences (Zehr et al., 2003). Strategies to mitigate and assess contamination exist, e.g.,
654 by employing ultrafiltration of reagents and including blanks at different stages of the sampling and sequencing process
655 (Bostrom et al., 2007; Farnelid et al., 2011; Blais et al., 2012; Moisander et al., 2014; Langlois et al., 2015; Fernandez-Mendez
656 et al., 2016; Cheung et al., 2021), but such strategies have not been universally adopted. Additionally, relative abundances of
657 PCR amplicons cannot easily be related to absolute abundances. For example, the relative abundance of a taxon can change
658 even if its absolute abundance remains constant, or the relative abundance can remain constant despite changes in the total
659 assemblage size. Moreover, the complexity of the diazotroph assemblage can, if the HTS sequencing depth is insufficient,
660 cause rare ASVs to go undetected, or have relative abundances which are too low to interpret.
661

662 Primary objectives in studying marine diazotrophic populations include understanding the contribution of each group to N₂
663 fixation, the factors influencing their activity, and their global distributions. The relative abundances of *nifH* genes and
664 transcripts estimated by the workflow can point to potentially significant contributors to N₂ fixation rates. Yet, the presence of
665 *nifH* genes or transcripts does not always correlate with N₂ fixation rates (e.g. (Gradoville et al., 2017)). This underscores the



666 need for cell-specific rates to better constrain N₂ fixation, the assemblages driving given rates, and the taxa-specific regulatory
667 factors of N₂ fixation to better constrain global biogeochemical modeling.

668
669 Various methods are available to target specific diazotroph taxa over space and time (e.g. qPCR/ddPCR, fluorescent in situ
670 hybridization (FISH)-based methods). Universal PCR assays, e.g., those used in the studies compiled here (*nifH*1-4), are an
671 important complement because they better capture the overall diversity of the diazotrophic assemblage. Unlike primers
672 designed for specific sequences, universal primers can amplify unknown or ambiguous sequences, enabling the discovery of
673 genetic diversity. This includes microdiversity, where sequences show subtle variations from known ones, or even identifying
674 entirely novel taxa. Primers specific to novel sequences can then be developed for use in the mentioned quantitative methods,
675 enabling experiments to characterize the growth, activity, and controlling factors/dynamics of putative diazotrophs growth.

676
677 Tools like RT-qPCR, where transcript abundances are assessed directly, or FISH-based methods where single-cells are
678 identified for cell-specific analysis, provide complementary perspectives into the activities of putative diazotrophs.
679 Enumerating diazotrophs using techniques like these can help standardize the relative abundances associated with amplicon
680 sequencing via matching taxa across each method. By assessing diversity and abundance simultaneously, major players can
681 potentially be identified and monitored.

682
683 Through genome reconstruction, `omics studies can enhance the characterization of putative diazotroph amplicon sequences
684 by providing a robust suite of associated genetic data, e.g., taxonomic, phylogenetic, and metabolic. Previous studies have led
685 to the assembly of dozens of diazotrophic genomes (Delmont et al., 2022; Delmont et al., 2018). However, `omics methods
686 often require massive amounts of data to detect rare community members, and linking genes of interest to other genomic
687 information, e.g., taxonomy, remains quite difficult. Gene-specific models are also required to retrieve diazotrophic
688 information and these models can benefit greatly from the high quality diazotrophic sequences of the *nifH* ASV database. In
689 summary, the complementary perspectives afforded by the methods just described should all be used to obtain robust insights
690 into diazotrophic assemblages.

691

692 **4 Data availability**

693 The *nifH* ASV database is freely available in Figshare (<https://doi.org/10.6084/m9.figshare.23795943.v1>; Morando et al.,
694 2024). HTS datasets for the 21 studies in the database can be obtained from the NCBI Sequence Read Archive using the NCBI
695 BioProject accessions in Table 1.



696 **5 Code availability**

697 The workflow used to generate the *nifH* ASV database is freely available in two GitHub repositories, one for the DADA2 *nifH*
698 pipeline (https://github.com/jdmagasin/nifH_amplicons_DADA2) and one for the post-pipeline stages
699 (<https://github.com/jdmagasin/nifH-ASV-workflow>; Morando et al., 2024).

700 **6 Conclusions**

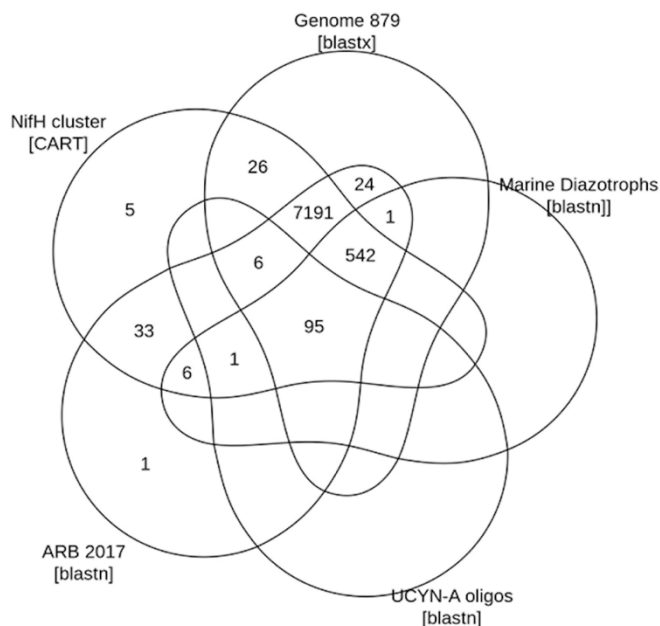
701 The workflow and *nifH* ASV database represent a significant step towards a unified framework that facilitates cross-study
702 comparisons of marine diazotroph diversity and biogeography. Furthermore, they could guide future research, including cruise
703 planning, e.g., focusing more on the southern hemisphere and areas outside of the tropics, and molecular assay development,
704 e.g., assays to characterize NCDs for single-cell activity rates.

705
706 To demonstrate the utility of our framework, the DNA dataset was used to identify potentially important ASVs and
707 diazotrophic groups, establishing global biogeographic patterns from this aggregated amplicon data. Cyanobacteria were the
708 dominant diazotrophic group, but cumulatively the NCDs made up more than half of the total data. Distinct latitudinal patterns
709 were seen among these major diazotrophic groups, with NCDs (clusters 1G, 1J/K, 1O/1P, 1A, and 3) having a greater
710 contribution to relative abundances near the equator and at higher latitudes, while cyanobacteria (1B) comprised a majority of
711 the diazotroph assemblage in the subtropics. SST appeared to restrict and differentiate the biogeography of clusters 1J/1K and
712 1O/1P (warm tropics/subtropics) from clusters 3 and 1A (cool, high latitude waters), but did not play as large of a role for the
713 biogeography of clusters 1B and 1G.

714
715 We provide the workflow and database for future investigations into the ecological factors driving global diazotrophic
716 biogeography and responses to a changing climate. Ultimately, we hope that insights derived from the use of our framework
717 will inform global biogeochemical models and improve predictions of future assemblages.

719 **Appendix A:**

720 Figures:



721

722

723

724

Figure A1. ASV annotations. The Venn diagram summarizes annotations assigned to 7931 ASVs during the AnnotateAuids stage of the workflow (Fig. 1). Numbers indicate how many ASVs received each type of annotation. Of the 9416 ASVs from the preceding workflow stage, FilterAuids, only the 7931 ASVs shown received annotations.

725

726

Tables:

727

728

729

Table A1. Compiled *nifH* amplicon studies. Information on all studies compiled to generate the *nifH* ASV database, as well as studies that were not ultimately included and the reasons for this. The table provides the study ID used to refer to each dataset, the NCBI BioProject accession, the number of samples, and the DOI of the publication in which the dataset became public.

Study ID	NCBI BioProject	Samples	Publication DOI	In <i>nifH</i> ASV DB?	Reason excluded
AK2HI	PRJNA1062410	43	This study	y	
NEMO	PRJNA1062391	56	This study	y	
Cabello 2020	PRJNA605009	75	10.1111/jpy.13045-20-043	n	Time series samples
Harding 2018	PRJNA476143	91	10.1073/pnas.1813658115	y	
Turk 2021	PRJNA695866	136	10.1038/s43705-021-00039-7	y	
Gradoville 2020 G1	PRJNA530276	111	10.1002/lno.11423	y	
Gradoville 2020 G2	PRJNA530276	56	10.1002/lno.11423	y	
Turk-Kubo 2015	PRJNA300416	11	10.5194/bg-12-7435-2015	n	Mesocosm samples
Farnelid 2019	PRJNA392595	155	10.1002/2017GB005681	n	
Shiozaki 2017	PRJDB5199	22	10.1002/lno.10933	y	
Shiozaki 2018LNO	PRJDB5679	20	10.1038/s41561-020-00651-7	y	
Shiozaki 2020	PRJDB9222	14	10.1029/2017GB005869	y	
Shiozaki 2018GBC	PRJDB6603	20	10.3389/fmicb.2018.00797	y	
Li 2018	PRJNA434503	16	10.1002/lno.10542	n	Issues merging reads
Gradoville 2017	PRJNA328516	49	10.1038/ismej.2014.119	y	
BentzonTilia 2015	PRJNA239310	56	10.3389/fmicb.2017.01122	y	
Gradoville 2017 Frontiers	PRJNA358796	45	10.1038/srep27858	n	Perturbation experiments



Rahav 2016	n/a	n/a	10.1038/s41396-018-0050-z	n	Samples were sorted prior to sequencing
Gerikas Ribeiro 2018	PRJNA377956	55	10.1038/nmicrobiol.2016.163	n	Samples contained very few sequences
MartinezPerez 2016	PRJNA326820	27	10.1029/2020JC017071	y	
Sato 2021	PRJDB10819	28	10.1002/lno.11727	y	
Selden 2021	PRJNA683637	10	10.1029/2018GB006130	y	
Mulholland 2018	PRJNA841982	29	10.1038/s41598-019-39586-4	y	
MoreiraCoello 2019	PRJNA473903	24	10.1007/s10021-021-00702-z	y	
TianjUni 2016	PRJNA637983	14	10.1007/s00248-019-01355-1	y	
TianjUni 2017	PRJNA438304	18	10.1002/lno.11997	y	
Hallstrom 2021	PRJNA656687	82	10.1007/s10533-022-00940-w	y	
Hallstrom 2022	PRJNA756869	83	10.3389/fmars.2020.00389	y	
Raes 2020	PRJNA385736	121	10.1038/s41396-020-0703-6	y	
Tang 2020	PRJNA554315	6	10.3390/biology10060555	y	
Ding 2021	SUB7406573	32	10.1007/s13131-019-1513-4	y	

730
731

732 Author Contributions

733 KTK and MM designed the study with input from SC and MMM. JM created and optimized the DADA2 pipeline for *nifH*
734 amplicon analyses. JM and MM developed the post-pipeline workflow. MM and JM compiled the database, retrieved
735 environmental data from CMAP, and analyzed the database. MM, JM and KTK wrote the manuscript with input from MMM,
736 SC, and JPZ.

737 Competing Interests

738 No competing interest is declared.

739 Acknowledgements

740 We gratefully acknowledge Mohammad Ashkezari and the Simons CMAP team, Stefan Green (Rush University) and the DNA
741 genomics core at University of Illinois at Chicago, Irina Shilova, Julie Robidart and Grace Reed for NEMO sampling and
742 sample processing, and Angelicque White (University of Hawaii, Manoa) and Mary R. Gradoville (Columbia River Inter-
743 Tribal Fish Commission) for AK2HI sampling and sample processing. We would like to thank the authors who directly
744 provided access to sequences: Takuhei Shiozaki (Shiozaki_2017 and Shiozaki_2018GBC) and Jun Sun, Changling Ding, and
745 Chao Wu (TianjUni_2016). This work was supported by grants from the National Science Foundation to KTK (OCE-2023498)
746 and the Simons Foundation to JPZ (Simons Collaboration on Ocean Processes and Ecology, Award ID 724220).
747



748 References

- 749 Angel, R., Nepel, M., Panholzl, C., Schmidt, H., Herbold, C. W., Eichorst, S. A., and Wobken, D.: Evaluation of Primers
750 Targeting the Diazotroph Functional Gene and Development of NifMAP - A Bioinformatics Pipeline for Analyzing nifH
751 Amplicon Data, *Front Microbiol*, 9, 703, 10.3389/fmicb.2018.00703, 2018.
- 752 Ashkezari, M. D., Hagen, N. R., Denholtz, M., Neang, A., Burns, T. C., Morales, R. L., Lee, C. P., Hill, C. N., and Armbrust,
753 E. V.: Simons Collaborative Marine Atlas Project (Simons CMAP): An open-source portal to share, visualize, and analyze
754 ocean data, *Limnol. Oceanogr.: Methods*, 19, 488-496, 2021.
- 755 Benavides, M., Conradt, L., Bonnet, S., Berman-Frank, I., Barrillon, S., Petrenko, A., and Dogliolii, A.: Fine-scale sampling
756 unveils diazotroph patchiness in the South Pacific Ocean, *ISME Communications*, 1, 3,
- 757 Bentzon-Tilia, M., Traving, S. J., Mantikci, M., Knudsen-Leerbeck, H., Hansen, J. L. S., Markager, S., and Riemann, L.:
758 Significant N₂ fixation by heterotrophs, photoheterotrophs and heterocystous cyanobacteria in two temperate estuaries, *ISME*
759 *J*, 9, 273-285, 2015.
- 760 Blais, M., Tremblay, J. É., Jungblut, A. D., Gagnon, J., Martin, J., Thaler, M., and Lovejoy, C.: Nitrogen fixation and
761 identification of potential diazotrophs in the Canadian Arctic, *Global Biogeochem. Cy.*, 26, GB3022, 10.1029/2011gb004096,
762 2012.
- 763 Bostrom, K. H., Riemann, L., Kuhl, M., and Hagstrom, A.: Isolation and gene quantification of heterotrophic N₂-fixing
764 bacterioplankton in the Baltic Sea, *Environ. Microbiol.*, 9, 152-164, doi:10.1111/j.1462-2920.2006.01124.x, 2007.
- 765 Cabello, A. M., Turk-Kubo, K. A., Hayashi, K., Jacobs, L., Kudela, R. M., and Zehr, J. P.: Unexpected presence of the nitrogen-
766 fixing symbiotic cyanobacterium UCYN-A in Monterey Bay, California, *J Phycol*, 56, 1521-1533, 10.1111/jpy.13045, 2020.
- 767 Callahan, B. J., McMurdie, P. J., Rosen, M. J., Han, A. W., Johnson, A. J., and Holmes, S. P.: DADA2: High-resolution sample
768 inference from Illumina amplicon data, *Nat Methods*, 13, 581-583, 10.1038/nmeth.3869, 2016.
- 769 Capone, D. G., Burns, J. A., Montoya, J. P., Subramaniam, A., Mahaffey, C., Gunderson, T., Michaels, A. F., and Carpenter,
770 E. J.: Nitrogen fixation by *Trichodesmium* spp.: An important source of new nitrogen to the tropical and subtropical North
771 Atlantic Ocean, *Global Biogeochem. Cy.*, 19, GB2024: 2021-2017, 2005.
- 772 Carpenter, E. J. and Capone, D. G.: Nitrogen in the marine environment, Academic Press, New York, 900 pp.1983.
- 773 Carpenter, E. J. and Foster, R. A.: Marine symbioses, in: *Cyanobacteria in Symbiosis*, edited by: Rai, A. N., Bergman, B., and
774 Rasmussen, U., Kluwer Academic Publishers, The Netherlands, 11-18, 2002.
- 775 Cheung, S., Xia, X., Guo, C., and Liu, H.: Diazotroph community structure in the deep oxygen minimum zone of the Costa
776 Rica Dome, *J Plankton Res*, 38, 380-391, 2016.
- 777 Cheung, S., Zehr, J. P., Xia, X., Tsurumoto, C., Endo, H., Nakaoka, S. I., Mak, W., Suzuki, K., and Liu, H.: Gamma4: a
778 genetically versatile Gammaproteobacterial *nifH* phylotype that is widely distributed in the North Pacific Ocean, *Environ*
779 *Microbiol*, 23, 4246-4259, 10.1111/1462-2920.15604, 2021.
- 780 Coale, T. H., Loconte, V., Turk-Kubo, K. A., Vanslebrouck, B., Mak, W. K. E., Cheung, S., Ekman, A., Chen, J. H., Hagino,
781 K., Takano, Y., Nishimura, T., Adachi, M., Le Gros, M., Larabell, C., and Zehr, J. P.: Nitrogen-fixing organelle in a marine
782 alga, *Science*, 384, 217-222, 10.1126/science.adk1075, 2024.



- 783 Delmont, T. O., Karlusich, J. J. P., Veseli, I., Fuessel, J., Eren, A. M., Foster, R. A., Bowler, C., Wincker, P., and Pelletier, E.:
784 Heterotrophic bacterial diazotrophs are more abundant than their cyanobacterial counterparts in metagenomes covering most
785 of the sunlit ocean, *ISME J*, 16, 927-936, 2022.
- 786 Delmont, T. O., Quince, C., Shaiber, A., Esen, Ö. C., Lee, S. T., Rappé, M. S., MacLellan, S. L., Lückner, S., and Eren, A. M.:
787 Nitrogen-fixing populations of Planctomycetes and Proteobacteria are abundant in surface ocean metagenomes, *Nature*
788 *microbiology*, 3, 804-813, 2018.
- 789 Ding, C., Wu, C., Li, L., Pujari, L., Zhang, G., and Sun, J.: Comparison of Diazotrophic Composition and Distribution in the
790 South China Sea and the Western Pacific Ocean, *Biology (Basel)*, 10, 10.3390/biology10060555, 2021.
- 791 Edgar, R.: UCHIME2: improved chimera prediction for amplicon sequencing, *BioRxiv*, doi.org/10.1101/074252, 2016.
- 792 Falcon, L., Cipriano, F., Chistoserdov, A., and Carpenter, E.: Diversity of diazotrophic unicellular cyanobacteria in the tropical
793 North Atlantic Ocean, *Appl Environ Microbiol*, 68, 5760, 2002.
- 794 Falcon, L., Carpenter, E., Cipriano, F., Bergman, B., and Capone, D.: N₂ fixation by unicellular bacterioplankton from the
795 Atlantic and Pacific Oceans: phylogeny and in situ rates, *Appl Environ Microbiol*, 70, 765-770, 2004.
- 796 Farnelid, H., Oberg, T., and Riemann, L.: Identity and dynamics of putative N₂-fixing picoplankton in the Baltic Sea proper
797 suggest complex patterns of regulation, *Environmental Microbiology Reports*, 1, 145-154, 10.1111/j.1758-2229.2009.00021.x,
798 2009.
- 799 Farnelid, H., Andersson, A. F., Bertilsson, S., Al-Soud, W. A., Hansen, L. H., Sørensen, S., Steward, G. F., Hagström, A., and
800 Riemann, L.: Nitrogenase gene amplicons from global marine surface waters are dominated by genes of non-cyanobacteria,
801 *PLOS ONE*, 6, e19223, 10.1371/journal.pone.0019223, 2011.
- 802 Fernandez, C., Farias, L., and Ulloa, O.: Nitrogen fixation in denitrified marine waters, *PLOS ONE*, 6, e20539,
803 10.1371/journal.pone.0020539, 2011.
- 804 Fernandez-Mendez, M., Turk-Kubo, K. A., Buttigieg, P. L., Rapp, J. Z., Krumpfen, T., Zehr, J. P., and Boetius, A.: Diazotroph
805 Diversity in the Sea Ice, Melt Ponds, and Surface Waters of the Eurasian Basin of the Central Arctic Ocean, *Front Microbiol*,
806 7, 1-18, 10.3389/fmicb.2016.01884, 2016.
- 807 Frank, I. E., Turk-Kubo, K. A., and Zehr, J. P.: Rapid annotation of *nifH* gene sequences using classification and regression
808 trees facilitates environmental functional gene analysis, *Env Microbiol Rep*, 8, 905-916, 2016.
- 809 Gaby, J. C. and Buckley, D. H.: A global census of nitrogenase diversity, *Environ Microbiol*, 13, 1790-1799, 10.1111/j.1462-
810 2920.2011.02488.x, 2011.
- 811 Goto, M., Ando, S., Hachisuka, Y., and Yoneyama, T.: Contamination of diverse *nifH* and *nifH*-like DNA into commercial
812 PCR primers, *FEMS Microbiol Lett*, 246, 33-38, 10.1016/j.femsle.2005.03.042, 2005.
- 813 Gradoville, M. R., Bombar, D., Crump, B. C., Letelier, R. M., Zehr, J. P., and White, A. E.: Diversity and activity of nitrogen-
814 fixing communities across ocean basins, *Limnol Oceanogr*, 62, 1895-1909, 2017.
- 815 Gradoville, M. R., Farnelid, H., White, A. E., Turk-Kubo, K. A., Stewart, B., Ribalet, F., Ferrón, S., Pinedo-Gonzalez, P.,
816 Armbrust, E. V., Karl, D. M., John, S., and Zehr, J. P.: Latitudinal constraints on the abundance and activity of the
817 cyanobacterium UCYN-A and other marine diazotrophs in the North Pacific, *Limnol Oceanogr*, 65, 1858-1875,
818 10.1002/lno.11423, 2020.



- 819 Green, S. J., Venkatramanan, R., and Naqib, A.: Deconstructing the polymerase chain reaction: Understanding and correcting
820 bias associated with primer degeneracies and primer-template mismatches, PLOS ONE, 10, e0128122,
821 doi:10.1371/journal.pone.0128122, 2015.
- 822 Hallstrøm, S., Benavides, M., Salamon, E. R., Arístegui, J., and Riemann, L.: Activity and distribution of diazotrophic
823 communities across the Cape Verde Frontal Zone in the Northeast Atlantic Ocean, Biogeochem, 1-19, 2022a.
- 824 Hallstrøm, S., Benavides, M., Salamon, E. R., Evans, C. W., Potts, L. J., Granger, J., Tobias, C. R., Moisander, P. H., and
825 Riemann, L.: Pelagic N₂ fixation dominated by sediment diazotrophic communities in a shallow temperate estuary, Limnol
826 Oceanogr, 67, 364-378, 2022b.
- 827 Halm, H., Lam, P., Ferdelman, T. G., Lavik, G., Dittmar, T., LaRoche, J., D'Hondt, S., and Kuypers, M. M.: Heterotrophic
828 organisms dominate nitrogen fixation in the South Pacific Gyre, ISME J, 6, 1238-1249, 10.1038/ismej.2011.182, 2012.
- 829 Harding, K., Turk-Kubo, K. A., Sipler, R. E., Mills, M. M., Bronk, D. A., and Zehr, J. P.: Symbiotic unicellular cyanobacteria
830 fix nitrogen in the Arctic Ocean, Proc Natl Acad Sci U S A, 115, 13371-13375, 10.1073/pnas.1813658115, 2018.
- 831 Heller, P., Tripp, H. J., Turk-Kubo, K., and Zehr, J. P.: ARBitrator: a software pipeline for on-demand retrieval of auto-curated
832 *nifH* sequences from GenBank, Bioinformatics, 10.1093/bioinformatics/btu417, 2014.
- 833 Jickells, T., Buitenhuis, E., Altieri, K., Baker, A., Capone, D., Duce, R., Dentener, F., Fennel, K., Kanakidou, M., and LaRoche,
834 J.: A reevaluation of the magnitude and impacts of anthropogenic atmospheric nitrogen inputs on the ocean, Global
835 Biogeochem. Cy., 31, 289-305, 2017.
- 836 Langlois, R., Großkopf, T., Mills, M., Takeda, S., and LaRoche, J.: Widespread distribution and expression of Gamma A
837 (UMB), an uncultured, diazotrophic, γ -proteobacterial *nifH* phylotype, PLOS ONE, 10, e0128912, 2015.
- 838 Langlois, R. J., LaRoche, J., and Raab, P. A.: Diazotrophic diversity and distribution in the tropical and subtropical Atlantic
839 Ocean, Appl Environ Microbiol, 71, 7910-7919, 10.1128/AEM.71.12.7910-7919.2005, 2005.
- 840 Liu, J., Zhou, L., Li, J., Lin, Y., Ke, Z., Zhao, C., Liu, H., Jiang, X., He, Y., and Tan, Y.: Effect of mesoscale eddies on
841 diazotroph community structure and nitrogen fixation rates in the South China Sea, Regional Studies in Marine Science, 35,
842 101106, 2020.
- 843 Löscher, C. R., Großkopf, T., Desai, F. D., Gill, D., Schunck, H., Croot, P. L., Schlosser, C., Neulinger, S. C., Pinnow, N., and
844 Lavik, G.: Facets of diazotrophy in the oxygen minimum zone waters off Peru, ISME J, 8, 2180-2192, 2014.
- 845 Luo, Y. W., Doney, S. C., Anderson, L. A., Benavides, M., Berman-Frank, I., Bode, A., Bonnet, S., Boström, K. H., Böttjer,
846 D., Capone, D. G., Carpenter, E. J., Chen, Y. L., Church, M. J., Dore, J. E., Falcón, L. I., Fernández, A., Foster, R. A., Furuya,
847 K., Gómez, F., Gundersen, K., Hynes, A. M., Karl, D. M., Kitajima, S., Langlois, R. J., LaRoche, J., Letelier, R. M., Marañón,
848 E., McGillicuddy, D. J., Moisander, P. H., Moore, C. M., Mouriño-Carballido, B., Mulholland, M. R., Needoba, J. A., Orcutt,
849 K. M., Poulton, A. J., Rahav, E., Raimbault, P., Rees, A. P., Riemann, L., Shiozaki, T., Subramaniam, A., Tyrrell, T., Turk-
850 Kubo, K. A., Varela, M., Villareal, T. A., Webb, E. A., White, A. E., Wu, J., and Zehr, J. P.: Database of diazotrophs in global
851 ocean: abundance, biomass and nitrogen fixation rates, Earth System Science Data, 4, 47-73, 10.5194/essd-4-47-2012, 2012.
- 852 Martin, M.: Cutadapt removes adapter sequences from high-throughput sequencing reads, EMBnet, 17, 10-12, 2011.
- 853 Messer, L. F., Mahaffey, C., Robinson, C. M., Jeffries, T. C., Baker, K. G., Isaksson, J. B., Ostrowski, M., Doblin, M. A.,
854 Brown, M. V., and Seymour, J. R.: High levels of heterogeneity in diazotroph diversity and activity within a putative hotspot
855 for marine nitrogen fixation, ISME J, 1499-1513, 2015.



- 856 Moisaner, P. H., Beinart, R. A., Voss, M., and Zehr, J. P.: Diversity and abundance of diazotrophic microorganisms in the
857 South China Sea during intermonsoon, *ISME J*, 2, 954-967, 10.1038/ismej.2008.51, 2008.
- 858 Moisaner, P. H., Serros, T., Paerl, R. W., Beinart, R. A., and Zehr, J. P.: Gammaproteobacterial diazotrophs and *nifH* gene
859 expression in surface waters of the South Pacific Ocean, *ISME J*, 8, 1962-1973, 10.1038/ismej.2014.49, 2014.
- 860 Moisaner, P. H., Benavides, M., Bonnet, S., Berman-Frank, I., White, A. E., and Riemann, L.: Chasing after non-
861 cyanobacterial nitrogen fixation in marine pelagic environments, *Front Microbiol*, 8, 1736, 2017.
- 862 Moonsamy, P. V., Williams, T., Bonella, P., Holcomb, C. L., Hoglund, B. N., Hillman, G., Goodridge, D., Turenchalk, G. S.,
863 Blake, L. A., Daigle, D. A., Simen, B. B., Hamilton, A., May, A. P., and Erlich, H. A.: High throughput HLA genotyping using
864 454 sequencing and the Fluidigm Access Array System for simplified amplicon library preparation, *Tissue Antigens*, 81, 141-
865 149, 10.1111/tan.12071, 2013.
- 866 Morando, M., Magasin, J., Cheung, S., Mills, M. M., Zehr, J. P., and Turk-Kubo, K. A.: *nifH* ASV database in Global
867 biogeography of N₂-fixing microbes: *nifH* amplicon database and analytics workflow, Figshare [dataset],
868 <https://doi.org/10.6084/m9.figshare.23795943.v1>, 2024.
- 869 Morando, M., Magasin, J., Cheung, S., Mills, M. M., Zehr, J. P., and Turk-Kubo, K. A.: DADA2 *nifH* pipeline in Global
870 biogeography of N₂-fixing microbes: *nifH* amplicon database and analytics workflow, GitHub [code],
871 https://github.com/jdmagasin/nifH_amplicons_DADA2, 2024.
- 872 Morando, M., Magasin, J., Cheung, S., Mills, M. M., Zehr, J. P., and Turk-Kubo, K. A.: *nifH* ASV workflow in Global
873 biogeography of N₂-fixing microbes: *nifH* amplicon database and analytics workflow, GitHub [code],
874 <https://github.com/jdmagasin/nifH-ASV-workflow>, 2024.
- 875 Mulholland, M. R., Bernhardt, P. W., Widner, B. N., Selden, C. R., Chappell, P. D., Clayton, S., Mannino, A., and Hyde, K.:
876 High Rates of N₂ Fixation in Temperate, Western North Atlantic Coastal Waters Expand the Realm of Marine Diazotrophy,
877 *Global Biogeochem. Cy.*, 33, 826-840, 10.1029/2018gb006130, 2019.
- 878 Pierella Karlusich, J. J., Pelletier, E., Lombard, F., Carsique, M., Dvorak, E., Colin, S., Picheral, M., Cornejo-Castillo, F. M.,
879 Acinas, S. G., Pepperkok, R., Karsenti, E., de Vargas, C., Wincker, P., Bowler, C., and Foster, R. A.: Global distribution
880 patterns of marine nitrogen-fixers by imaging and molecular methods, *Nat Commun*, 12, 1-18, 10.1038/s41467-021-24299-y,
881 2021.
- 882 Raes, E. J., Van de Kamp, J., Bodrossy, L., Fong, A. A., Riekenberg, J., Holmes, B. H., Eler, D. V., Eyre, B. D., Weil, S. S.,
883 and Waite, A. M.: N₂ fixation and new insights into nitrification from the ice-edge to the equator in the South Pacific Ocean,
884 *Frontiers in Marine Science*, 7, 1-20, 2020.
- 885 Rho, M., Tang, H., and Ye, Y.: FragGeneScan: predicting genes in short and error-prone reads, *Nucleic Acids Res*, 38, e191,
886 10.1093/nar/gkq747, 2010.
- 887 Rognes, T., Flouri, T., Nichols, B., Quince, C., and Mahe, F.: VSEARCH: a versatile open source tool for metagenomics,
888 *PeerJ*, 4, e2584, 10.7717/peerj.2584, 2016.
- 889 Sato, T., Shiozaki, T., Taniuchi, Y., Kasai, H., and Takahashi, K.: Nitrogen Fixation and Diazotroph Community in the
890 Subarctic Sea of Japan and Sea of Okhotsk, *Journal of Geophysical Research: Oceans*, 126, e2020JC017071, 2021.



- 891 Selden, C. R., Chappell, P. D., Clayton, S., Macías-Tapia, A., Bernhardt, P. W., and Mulholland, M. R.: A coastal N₂ fixation
892 hotspot at the Cape Hatteras front: Elucidating spatial heterogeneity in diazotroph activity via supervised machine learning,
893 *Limnol Oceanogr*, 66, 1832-1849, 2021.
- 894 Shao, Z. and Luo, Y. W.: Controlling factors on the global distribution of a representative marine heterotrophic diazotroph
895 phylotype (Gamma A), *Biogeosciences*, 19, 2939-2952, 2022.
- 896 Shao, Z., Xu, Y., Wang, H., Luo, W., Wang, L., Huang, Y., Agawin, N. S. R., Ahmed, A., Benavides, M., Bentzon-Tilia, M.,
897 and Berman-Frank, I.: Global Oceanic Diazotroph Database Version 2 and Elevated Estimate of Global N₂ Fixation, *Earth
898 System Science Data*, 15, 2023.
- 899 Shilova, I., Mills, M., Robidart, J., Turk-Kubo, K., Björkman, K., Kolber, Z., Rapp, I., van Dijken, G., Church, M., and Arrigo,
900 K.: Differential effects of nitrate, ammonium, and urea as N sources for microbial communities in the North Pacific Ocean,
901 *Limnol Oceanogr*, 62, 2550-2574, 2017.
- 902 Shiozaki, T., Fujiwara, A., Inomura, K., Hirose, Y., Hashihama, F., and Harada, N.: Biological nitrogen fixation detected under
903 Antarctic sea ice, *Nature Geoscience*, 13, 729–732, 2020.
- 904 Shiozaki, T., Fujiwara, A., Ijichi, M., Harada, N., Nishino, S., Nishi, S., Nagata, T., and Hamasaki, K.: Diazotroph community
905 structure and the role of nitrogen fixation in the nitrogen cycle in the Chukchi Sea (western Arctic Ocean), *Limnol Oceanogr*,
906 63, 2191-2205, 10.1002/lno.10933, 2018a.
- 907 Shiozaki, T., Bombar, D., Riemann, L., Hashihama, F., Takeda, S., Yamaguchi, T., Ehama, M., Hamasaki, K., and Furuya,
908 K.: Basin scale variability of active diazotrophs and nitrogen fixation in the North Pacific, from the tropics to the subarctic
909 Bering Sea, *Global Biogeochem. Cy.*, 31, 996-1009, 10.1002/2017gb005681, 2017.
- 910 Shiozaki, T., Bombar, D., Riemann, L., Sato, M., Hashihama, F., Kodama, T., Tanita, I., Takeda, S., Saito, H., Hamasaki, K.,
911 and Furuya, K.: Linkage between dinitrogen fixation and primary production in the oligotrophic South Pacific Ocean, *Global
912 Biogeochem. Cy.*, 32, 1028-1044, 2018b.
- 913 Tang, W., Li, Z., and Cassar, N.: Machine learning estimates of global marine nitrogen fixation, *Journal of Geophysical
914 Research: Biogeosciences*, 124, 717-730, 2019.
- 915 Tang, W., Cerdan-Garcia, E., Berthelot, H., Polyviou, D., Wang, S., Baylay, A., Whitby, H., Planquette, H., Mowlem, M.,
916 Robidart, J., and Cassar, N.: New insights into the distributions of nitrogen fixation and diazotrophs revealed by high-resolution
917 sensing and sampling methods, *ISME J*, 14, 2514-2526, 10.1038/s41396-020-0703-6, 2020.
- 918 Taylor, L. J., Abbas, A., and Bushman, F. D.: grabseqs: Simple downloading of reads and metadata from multiple next-
919 generation sequencing data repositories, *Bioinformatics*, doi.org/10.1093/bioinformatics/btaa167, 2020.
- 920 Turk, K., Rees, A. P., Zehr, J. P., Pereira, N., Swift, P., Shelley, R., Lohan, M., Woodward, E. M. S., and Gilbert, J.: Nitrogen
921 fixation and nitrogenase (*nifH*) expression in tropical waters of the eastern North Atlantic, *ISME J*, 5, 1201-1212,
922 10.1038/ismej.2010.205, 2011.
- 923 Turk-Kubo, K. A., Karamchandani, M., Capone, D. G., and Zehr, J. P.: The paradox of marine heterotrophic nitrogen fixation:
924 abundances of heterotrophic diazotrophs do not account for nitrogen fixation rates in the Eastern Tropical South Pacific,
925 *Environ Microbiol*, 16, 3095-3114, 10.1111/1462-2920.12346, 2014.



- 926 Turk-Kubo, K. A., Farnelid, H. M., Shilova, I. N., Henke, B., and Zehr, J. P.: Distinct ecological niches of marine symbiotic
927 N₂-fixing cyanobacterium *Candidatus Atelocyanobacterium thalassa* sublineages, *J Phycol*, 53, 451-461, 10.1111/jpy.12505,
928 2017.
- 929 Turk-Kubo, K. A., Gradoville, M. R., Cheung, S., Cornejo-Castillo, F., Harding, K. J., Morando, M., Mills, M., and Zehr, J.
930 P.: Non-cyanobacterial diazotrophs: Global diversity, distribution, ecophysiology, and activity in marine waters, *FEMS*
931 *Microbiol Rev*, 10.1093/femsre/fuac046, 2022.
- 932 Turk-Kubo, K. A., Mills, M. M., Arrigo, K. R., van Dijken, G., Henke, B. A., Stewart, B., Wilson, S. T., and Zehr, J. P.:
933 UCYN-A/haptophyte symbioses dominate N₂ fixation in the Southern California Current System, *ISME Communications*, 1,
934 1-13, 2021.
- 935 Villareal, T. A.: Widespread occurrence of the *Hemiaulus*-cyanobacterial symbiosis in the southwest North-Atlantic Ocean,
936 *Bulletin of Marine Science*, 54, 1-7, 1994.
- 937 Wu, C., Kan, J., Liu, H., Pujari, L., Guo, C., Wang, X., and Sun, J.: Heterotrophic Bacteria Dominate the Diazotrophic
938 Community in the Eastern Indian Ocean (EIO) during Pre-Southwest Monsoon, *Microb Ecol*, 78, 804-819, 10.1007/s00248-
939 019-01355-1, 2019.
- 940 Wu, C., Sun, J., Liu, H., Xu, W., Zhang, G., Lu, H., and Guo, Y.: Evidence of the Significant Contribution of Heterotrophic
941 Diazotrophs to Nitrogen Fixation in the Eastern Indian Ocean During Pre-Southwest Monsoon Period, *Ecosyst*, 25, 1066-1083,
942 2021.
- 943 Zani, S.: Application of a nested reverse transcriptase polymerase chain reaction assay for the detection of *nifH* expression in
944 Lake George, New York, M. S. Thesis, Rensselaer Polytechnic Institute, 1999.
- 945 Zehr, J. and McReynolds, L.: Use of degenerate oligonucleotides for amplification of the *nifH* gene from the marine
946 cyanobacterium *Trichodesmium thiebautii*, *Appl Environ Microbiol*, 55, 2522-2526, 1989.
- 947 Zehr, J., Mellon, M., and Zani, S.: New nitrogen-fixing microorganisms detected in oligotrophic oceans by amplification of
948 nitrogenase (*nifH*) genes, *Appl. Environ. Microbiol*, 64, 3444-3450, 1998.
- 949 Zehr, J. P. and Capone, D. G.: Changing perspectives in marine nitrogen fixation, *Science*, 368, eaay9514,
950 10.1126/science.aay9514, 2020.
- 951 Zehr, J. P., Crumbliss, L. L., Church, M. J., Omoregie, E. O., and Jenkins, B. D.: Nitrogenase genes in PCR and RT-PCR
952 reagents: implications for studies of diversity of functional genes, *Biotechniques*, 35, 996-1005, 2003.
- 953 Zehr, J. P., Waterbury, J. B., Turner, P. J., Montoya, J. P., Omoregie, E., Steward, G. F., Hansen, A., and Karl, D. M.:
954 Unicellular cyanobacteria fix N₂ in the subtropical North Pacific Ocean, *Nature*, 412, 635-638, 2001.
955